# Cyclic Erosional Instability of Sandbars along the Colorado River, Grand Canyon, Arizona

Leland R. Dexter* and Brian L. Cluer**

*Department of Geography, Northern Arizona University
**Water Resources Division, National Park Service

The study and management of regulated rivers have become important issues. A prime example is Glen Canyon Dam and its operational impacts on the downstream environment in Grand Canyon National Park, Arizona. We present an overview of the Glen Canyon Dam environmental issue, a novel methodology for monitoring dam impacts on alluvial sediments, and three years of study relating to the stability of alluvial deposits along the Colorado River. This research uses oblique photographs taken daily, automatically, from twenty-one fixed-position programmable cameras. Digital image-processing techniques created planimetric models of sandbar area from the photos for the period of March 1993 through May 1995. The technique allowed daily tracking of sandbar areas for detection of rapid erosional events. We demonstrated that rapid erosional events occur commonly on Grand Canyon sandbars. Sandbars are unstable over the study period, especially the first two years. Most of the rapid erosional events are associated with weekend or seasonal reduction in flow. Sandbar area frequency is bimodal with negative kurtosis, indicating that measurements taken at long time-steps are not likely to document mean area but rather minima or maxima. Time-series analysis suggests that periods of relative stability occur between rapid area-reducing events. Sandbars appear to adjust in two modes, a short-term adjustment mode occurring over hours and a long-term adjustment mode over days to weeks. The understanding and minimization of rapid-failure events should be increased, and the phenomenon needs to be addressed in any comprehensive sediment management plan. *Key Words: sandbar, fluvial erosion, image analysis, Colorado River, Grand Canyon National Park, Glen Canyon Dam.*

May 1996 began a new era in the operation of U.S. dams when Secretary of the Interior Bruce Babbitt signed a record of decision (ROD) concluding an environmental impact assessment process that had spanned more than a decade (U.S. Bureau of Reclamation 1995). The decision specified that Glen Canyon Dam on the Colorado River would be operated under a set of temporary and adaptive flow criteria termed the "Interim Flow Prescription" (described in detail below). The dam would no longer be operated just for power generation, but would also be used to reduce impacts on the downstream riparian environment, with provisions to allow for periodic rejuvenating flood releases. The ROD followed a much-publicized Test Flood released from Glen Canyon Dam between March 26 and April 4, 1996. A major objective of this "engineered" flood was to translocate sand from the riverbed onto the adjacent banks in an attempt to rebuild the sandbars in Grand Canyon National Park, which are valuable resources for plants, fish, birds, and other canyon life. Success of the flood for sandbar regeneration was immediately apparent. Nevertheless, the longevity of the elevated sand deposits is still unknown, as is the "optimal" long-term dam-release strategy.

In this paper, we present an overview of the Glen Canyon Dam environmental impact assessment process, a novel methodology for short-term monitoring of impacts to river sediments, and three years of pre-flood, interim flow results. The data suggest that many Grand Canyon sandbars are prone to very short-term erosional episodes that appear to be closely coupled to dam operation. An "optimal" management strategy will therefore need to accommodate both long-term and short-term attributes of this fluvial system.

*Annals of the Association of American Geographers*, 89(2), 1999, p. 238–266
©1999 by Association of American Geographers
Published by Blackwell Publishers, 350 Main Street, Malden, MA 02148, and 108 Cowley Road, Oxford, OX4 1JF, UK.

## Overview

Classical concepts in fluvial geomorphology were developed around natural, unregulated river systems (Gilbert 1876, 1877; Davis 1899, 1902; Hack 1960, 1975; Leopold and Langbein 1962; Langbein and Leopold 1964; Schumm 1977). The few remaining unregulated rivers in the western U.S. are typically characterized by highly variable discharge, dominated by an annual snowmelt-driven spring flood that mobilizes large amounts of sediment. Regulated rivers, on the other hand, are characterized by less variable discharge, reduced flood frequency, impoundment of sediment upstream of dams, and enhanced erosion downstream of dams (Williams and Wolman 1984; Collier et al. 1996; Graf 1996).

Before the 1960s, the federal government built dams on rivers as key elements in policies fostering national economic growth. These policies justified dams on the basis of providing water resources, hydroelectric power, flood control, and recreation. Once the dams were in place, economic concerns almost completely governed the operating schedule (Bureau of Reclamation 1995). Upstream environments were sacrificed to reservoir impoundment, regardless of scenic grandeur or preexisting human use. Rising reservoir levels threatened even unique scenic landmarks like Rainbow Bridge, a large sandstone natural bridge across a tributary canyon of the Colorado River in Utah (Figure 1). Very little, if any, consideration was given to the effects of dam operation on the downstream environment, even if that area included a major national park established to preserve the natural environment within its bounds. Indeed, the impacts of human-induced flow regulation on downstream environments were not widely studied until the 1970s (Ingram et al. 1991).

Since the 1970s, attitudes about river regulation have been changing in the U.S. Proposed and existing dams have come under attack on several fronts, especially for the effects of flow regulation on rapidly diminishing, natural riverine environments. Concurrent with these expressions of concerns, research in the field of geomorphology has shifted toward more applied problems (Graf 1996). As a consequence, considerable effort is now directed to the geomorphology of regulated fluvial systems (Howard 1975; Howard and Dolan 1979; Williams and Wolman 1984; Graf 1985, 1992, 1996; Leopold 1991; Wegner 1991; Beus 1992; Beus and Avery 1992; Collier et al. 1996).

The Colorado River has earned the dubious distinction of being the most heavily regulated river of its size in the world (Weatherford and Brown 1983). Along the combined Green and Colorado Rivers, ten major dams were constructed between 1931 and 1963, the last one on the mainstem Colorado being Glen Canyon (Figures 1, 2). Strategically sited to facilitate the apportionment mandates of the 1922 Colorado River Compact, Glen Canyon Dam was constructed between 1956 and 1963. In March 1963, the river diversion works were closed, and Lake Powell began filling (Figure 2). Since then, the operation of Glen Canyon Dam has profoundly influenced the downstream riparian environment throughout Grand Canyon National Park (Dolan et al. 1974; Andrews 1991; Dawdy 1991; Johnson 1991) (Figure 3).

Operational policy for Glen Canyon Dam was not originally evaluated in terms of its impact on the downstream environment. In fact, the age of the dam made it exempt from National Environmental Protection Act (NEPA) scrutiny. This situation changed following a lawsuit by river users (Graf 1996), filed at a time when the Bureau of Reclamation expressed interest in upgrading the infrastructure of the dam (Bureau of Reclamation 1995). From 1982 through 1996, numerous environmental studies assessed the types and magnitudes of changes downstream of Glen Canyon Dam. The Bureau of Reclamation's Glen Canyon Environmental Studies (GCES) office coordinated these studies (National Academy of Science 1987; Wegner 1991), which culminated in the compilation of an environmental impact statement (EIS). Following the enactment of the ROD in May 1996, the Bureau turned management of related studies over to the Grand Canyon Monitoring and Research Center (GCMRC).

### Effects of Glen Canyon Dam on Colorado River Hydrology

The most noticeable difference in flow regime of the Colorado River resulting from operations of Glen Canyon Dam is the change from an annual flow cycle (ranging between approximately 2850 cms – 50 cms) to a diurnal flow cycle (ranging between approximately 850 cms – 225 cms). A snowmelt-driven flood, usually peaking in late May or June, dominated the natural annual

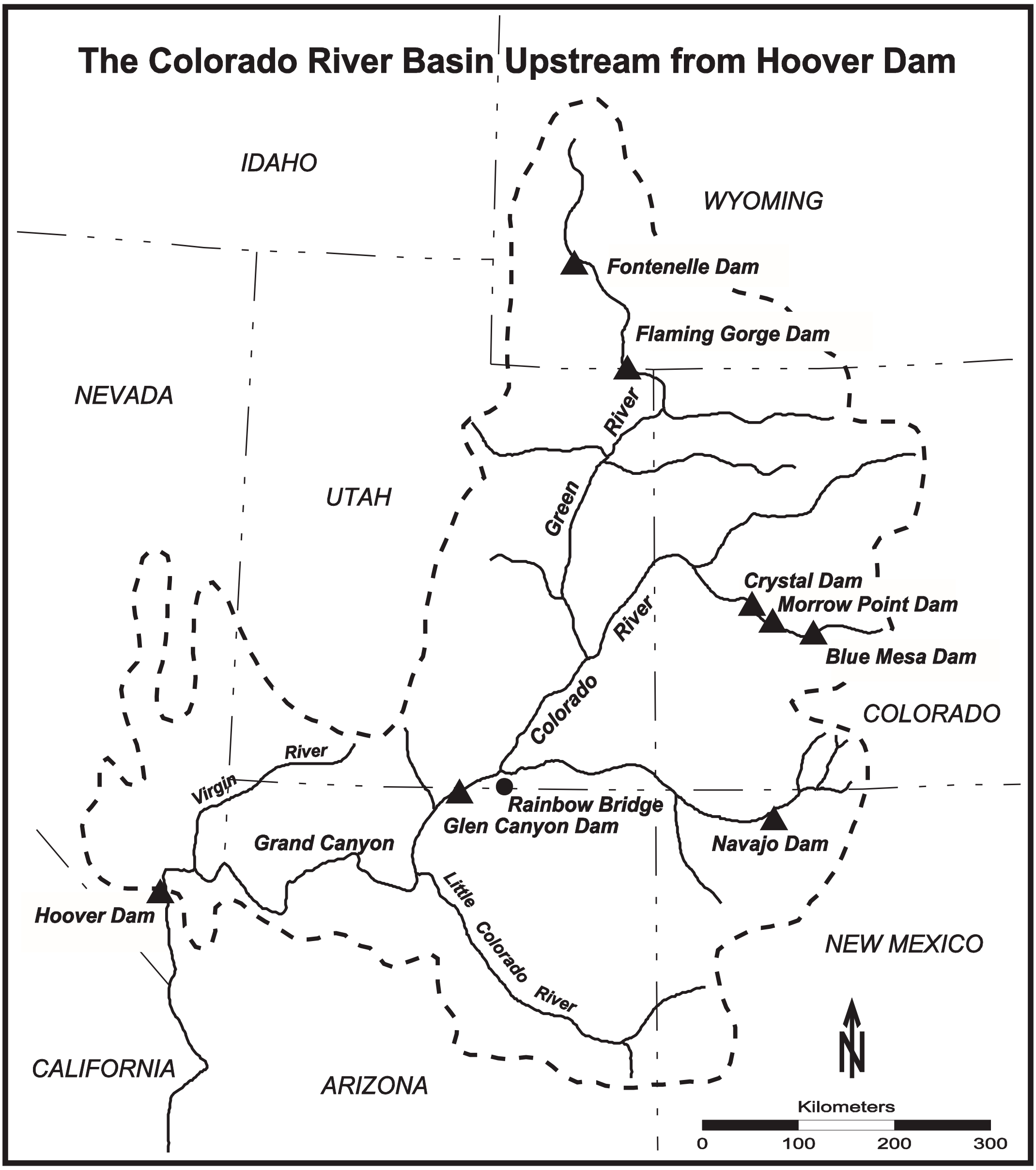


**Figure 1.** Regional index map showing the Colorado River Basin upstream from Hoover Dam.

flow cycle (Figure 3). Since the completion of Glen Canyon Dam, demand for electric power generation has mainly determined water releases. Like most other power-producing dams, Glen Canyon operates as a "peaking-power" facility because hydroelectric power output can be changed easily to meet demand. The most common peak-power demands result from midday summer air conditioning and nightly winter heating. Peak electrical power demand is highest in the summer, lowest in the spring and fall, and slightly elevated in the winter, and discharge releases vary accordingly (Figure 4). Discharges in excess of powerplant capacity (approximately 880 cms) have occurred only during rare facilities tests or emergency conditions. The March 1996 test flood, for example, was run at 1275 cms (45,000 cfs).

Beginning in June 1990, operators modified the water releases from Glen Canyon Dam to

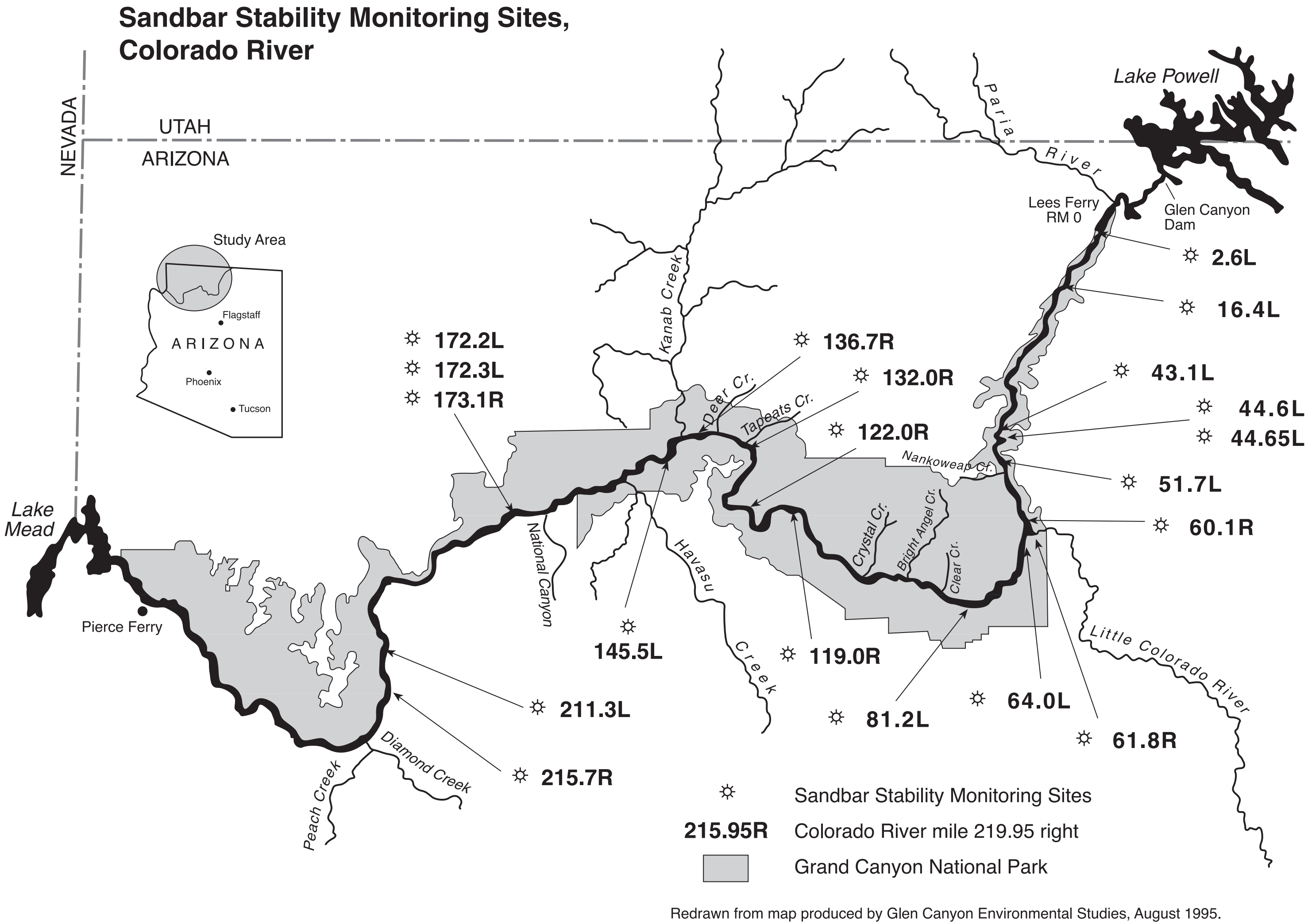


**Figure 2.** Grand Canyon area and sandbar photography site index map (courtesy Glen Canyon Environmental Studies).

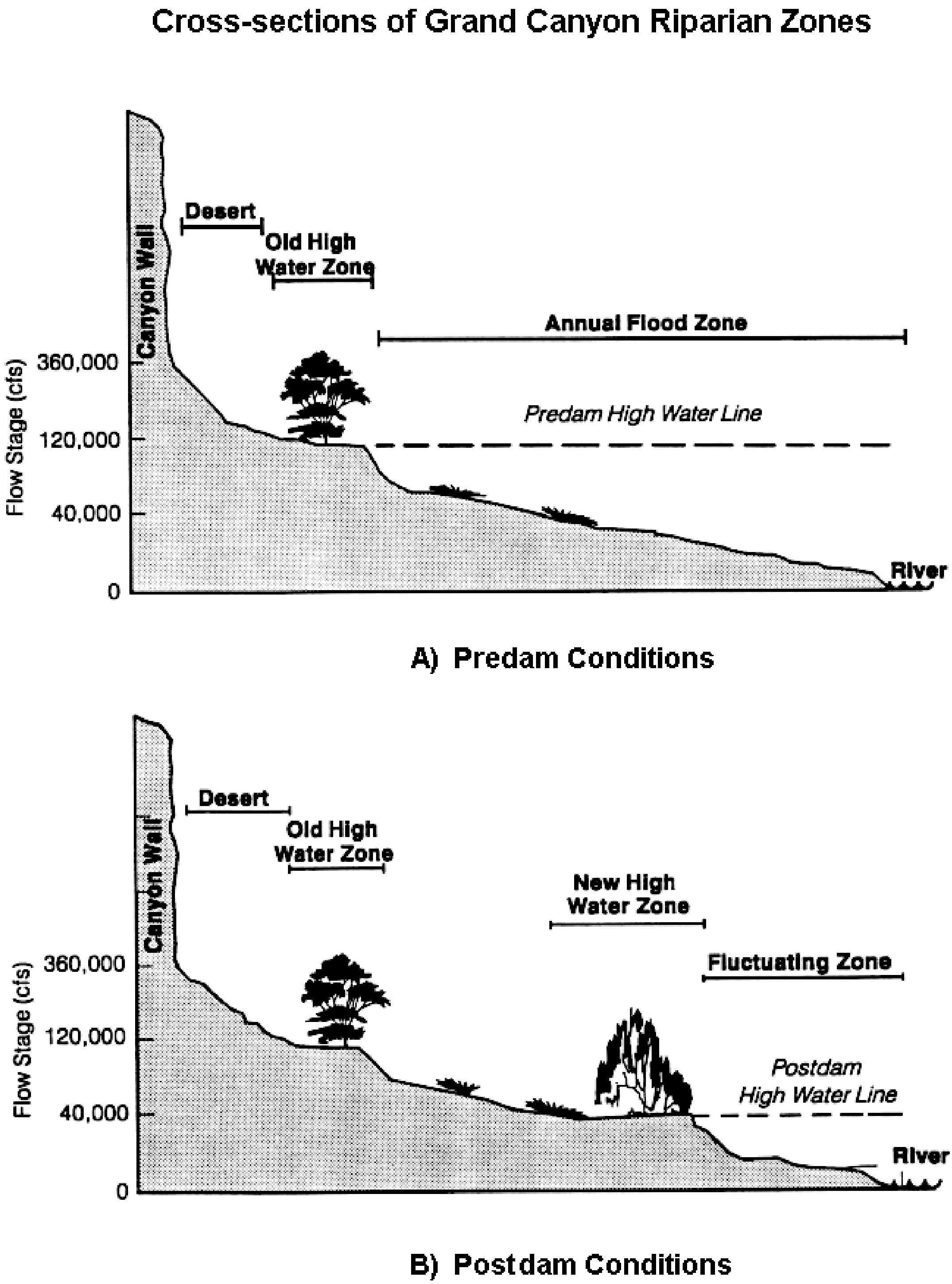


**Figure 3.** Cross-sections of Grand Canyon riparian zones: (a) predam (before 1963); and (b) postdam (after 1963) (from U.S. Bureau of Reclamation 1995).

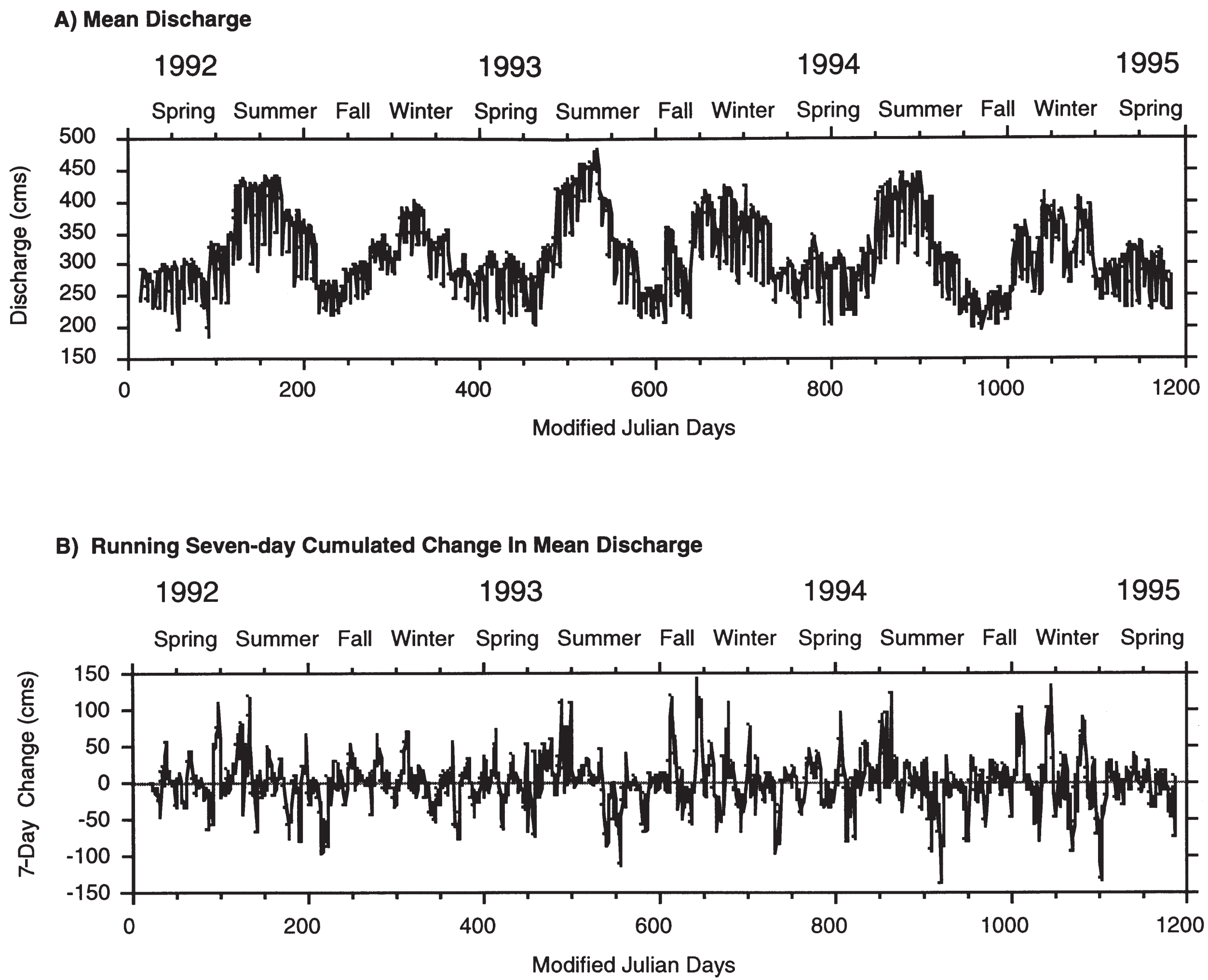


**Figure 4.** Time-series plots of (a) mean discharge and (b) running seven-day cumulated change in mean discharge from Glen Canyon Dam for the study period. Modified Julian day number one is March 1, 1992.

include a series of research-oriented GCES Phase Two Test Flows. Based on initial conclusions derived from these flows, they modified the operation schedule to reduce impacts on downstream riparian environments, and since August 1991 (and during the course of this research), Glen Canyon Dam has been operating under the so-called "Interim Flow Prescription." Under this prescription, the maximum allowable release from Glen Canyon Dam is 567 cms (20,000 cfs). The minimum allowable release ranges from 142 cms (5,000 cfs) for up to six hours at night to 227 cms (8,000 cfs) from 7 a.m. to 7 p.m. The allowable change per day is 142 cms (5,000 cfs) for low-volume months, 170 cms (6,000 cfs) for medium-volume months, and 227 cms (8,000 cfs) for high-volume months. Ramping rates (changes in discharge) are also constrained. Upramping (i.e., increases in discharge) must not exceed 227 cms (8,000 cfs) over a four-hour period with a maximum of 71 cms/h (2,500 cfs/h). Downramping (i.e., decreases in discharge) must not exceed –71 cms/h (–2,500 cfs/h). While a diurnal kinematic wave is still imparted to the downstream discharge, the peak amplitude and ramping rates (especially the downramp) are more constrained than in the past. The residence time of a single-day kinematic wave within the length of Grand Canyon is about three days. As a new crest is released from the dam (river mile minus 10), the previous crest is near Phantom Ranch (approximately river mile 88), another is near Mohawk Canyon (approximately river mile 171), and the last crest is in the lower end of Grand Canyon (approximately river mile 235). As each kinematic wave progresses downstream, the wave amplitude and wavelength decrease slightly (Dawdy 1991). In addition to the daily fluctuations in discharge, current operation of the powerplant induces a weekly (Figure 5) and annual signature. The weekly "wave" occurs due to reduced peak-power demands on weekends, while the annual signature is due to seasonal changes in peak-power demand. The effects of hydrologic cycling at these longer time steps have been much less intensely studied, and yet may have an effect on the stability of sandbars (Cluer 1995).

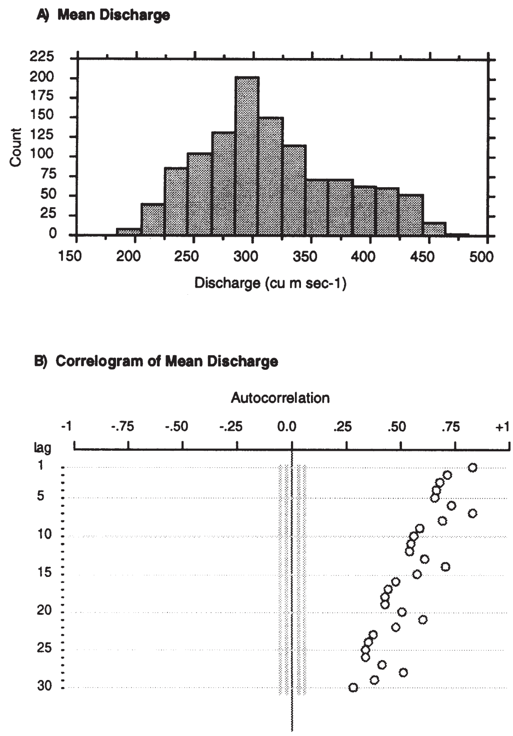


**Figure 5.** Frequency histogram (a) and autocorrelation correlogram (b) for mean discharge from Glen Canyon Dam for the study period. Peaks in the correlogram at successive harmonics of seven days indicate weekend reduction in discharge.

## Colorado River Sediment Resources

Although the Colorado River flows through a primarily bedrock gorge in the Grand Canyon, sandbars and other fluvial deposits are extremely important components of the river ecosystem. Sandbars serve as substrate for vegetation (Johnson 1991), as material for water-stilling and water-warming structures used by aquatic fauna (Valdez and Williams 1993), and as camping sites for river runners (Dolan et al. 1974). The fluvial sediment resources of the system have been a major emphasis of the GCES and GCMRC investigations. Sediment delivery from tributaries, the dynamics of sediment transport, and sediment storage are important factors that must be included in management plans. Indeed, the fluvial sediment resource is the first management priority of the Colorado River Management Plan (U.S. NPS 1989). This plan is due for revision, but sediment will probably retain high priority in the new plan.

Howard and Dolan (1981) classify the fluvial sediment resources of the Grand Canyon based on three general particle sizes and associated time-scales of mobility. In their scheme, the largest size category includes bedrock and large boulders, which are mobilized only over cyclic time-scales (Schumm 1977) of tens of thousands of years during extreme floods. There is evidence suggesting that flooding in excess of 8,700 cms (300,000 cfs) has occurred (Collier et al. 1996). The intermediate particle-size category includes gravel and cobbles that are mobilized during smaller floods. Since the closure of Glen Canyon Dam these floods have occurred very infrequently and only under exceptional circumstances. Examples of such floods include the emergency spill from Glen Canyon Dam in 1983 that exceeded 2,600 cms (90,000 cfs), the natural tributary flood from the Little Colorado River in 1993, and the engineered Test Flood in 1996. The finest particle-size category includes sand, silt, and clay, with "sand" being the name applied to this class by Howard and Dolan (1981). Sediment of the "sand" particle-size has been the focus of three decades of study and semicontinuous monitoring. Sand is mobile, or potentially mobile, under most flow conditions. Sand responds to dam releases and records cause-and-effect relationships resulting from dam operations. Sand delivery has been significantly reduced because flood water and sediments are held behind Glen Canyon Dam. The postdam supply of sand is limited to that stored in and along the channel below the dam and that introduced from ephemeral tributaries, both of which are difficult to measure (Andrews 1991). Smillie et al. (1993) estimated that the balance between sand supply and transport can be a deficit or a surplus depending on operation of the power plant.

We will refer to all fluvial sand deposits, regardless of geomorphic position or genesis, as "sandbars" in order to reduce confusion over terminology. Sandbars form in zones of low velocity that are created by irregularities and interruptions in the channel profile (Figure 6). Constrictions of the channel cause local acceleration of flow velocity, resulting in "supercritical" or "shooting" flow that creates rapids. The accelerated flow "separates" from the bank at the apex of the channel constriction. A low-velocity, recirculating "eddy" occurs downstream of the constriction in the separation zone. An "eddy fence" forms as a narrow zone of strong shear between the shooting flow and the eddy (Kieffer 1985). When the shooting flow of the rapid decelerates, flow "reattaches" to the bank at some point downstream (Schmidt 1990). The deposits that usually result are shown under low-stage conditions in Figure 6 (after Schmidt and Graf 1990). Typically, sandbars are found along the upstream face of channel constrictions (upper pool bars), along the downstream face of channel constrictions (separation bars), in the quiet water of the eddy center (eddy bars), and at the stagnation zone of the flow attachment (reattachment bars). Less common depositional environments include point bars on the inside of meanders and thin channel-margin sandbars between outcrops of bedrock or large boulders.

The mechanisms by which sandbars change form and size are of interest to scientists as well as resource managers and planners. Three major mechanisms are active in the reworking of sandbars. These mechanisms include seepage-induced failure during low flow, wave-induced erosion from surface turbulence, and drag forces from bottom turbulence and downstream flow (Carpenter et al. 1991, 1995; Budhu 1992; Bauer and Schmidt 1993; Werrell et al. 1993; Budhu and Gobin 1994). The greatest impact of dam operation on downstream sediment resources is the replacement of large annual floods that replenish sediments at relatively high elevations along the channel margins, with numerous daily "kinematic waves" of low amplitude that now nick away the base of the deposits (Figure 3).

## Geomorphic Equilibrium and Sandbar Stability

Much has been written about the notions of stability and the broader concept of equilibrium (see Thorn and Welford 1994 for an interesting discussion of the concept[s] of equilibrium as applied to geomorphology). In terms of the fluvial sandbars investigated here, there are at least two definitions of stability that could be invoked. One definition considers sandbars as stable-form features that occur in the same place and display the same general shape through time, but allow dynamic mass fluxes. Grand Canyon sandbars generally do occur in predictable locations, based on the interaction between river hydraulics and less mobile controlling features such as bedrock or boulders (Schmidt 1990). Sandbars have been observed in many of these locations over the length of historical record (Webb 1996). This definition, however, leaves the important aspect of "permanence" unanswered. Does the dynamically reworked sediment simply cycle back and forth between subaqueous eddy pools and subaerial sandbars, or does sediment move downstream

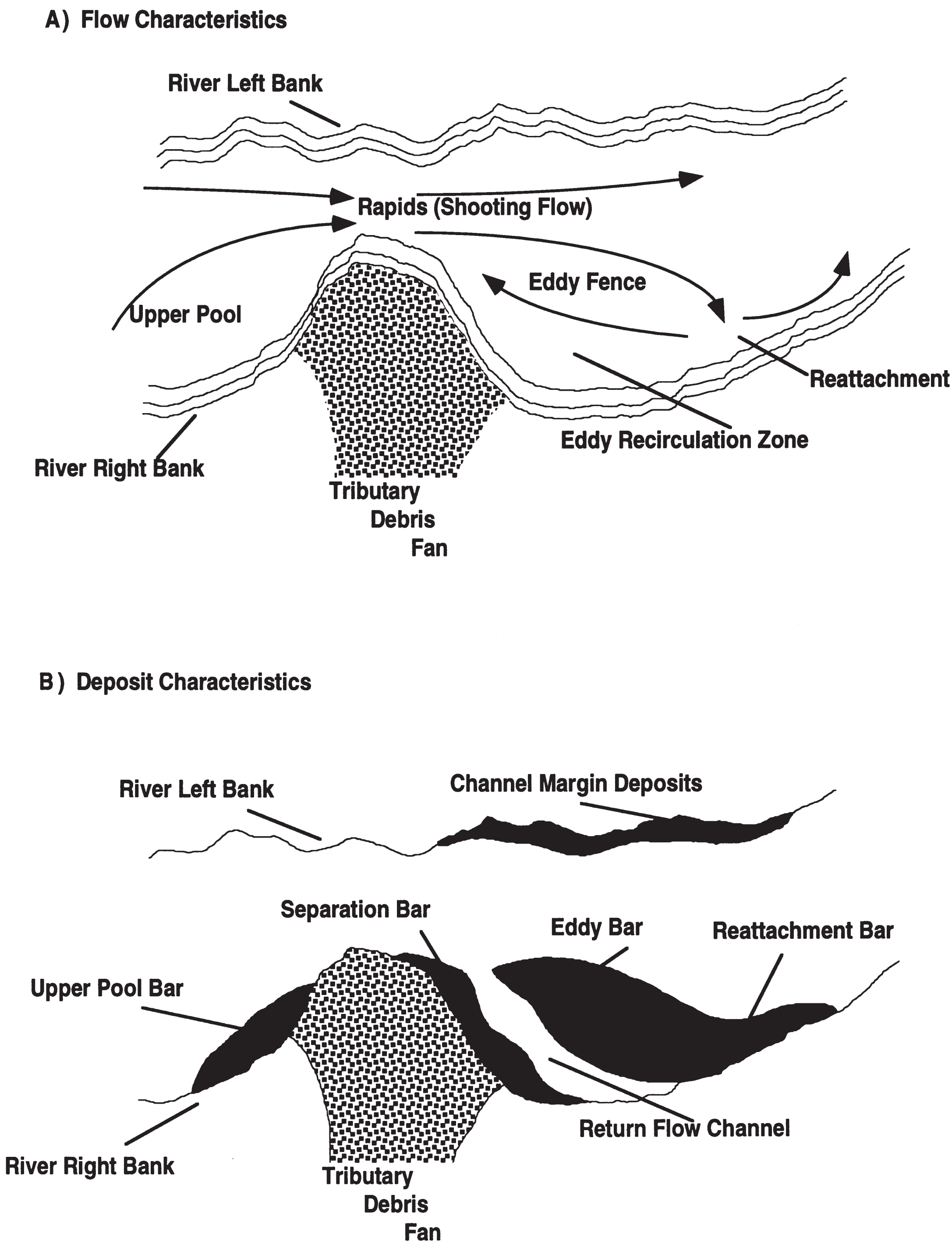


**Figure 6.** Characteristics of Grand Canyon sandbars. The top panel (a) illustrates the major hydraulic components of a rapid shown at high water. The bottom panel (b) illustrates the resulting alluvial deposits shown at low water (after Schmidt and Graf 1990).

with each reworking cycle? The answer to this question is crucial in understanding and controlling rates of sediment movement through what has become a "sediment-starved" system.

A second, much stricter definition would treat stability with respect to both mass flux and bar form. Under this definition, every particle of sand remains in more or less the same location over some defined time period. While this notion of stability becomes progressively unrealistic over increasingly long time increments, river managers would like to simulate this ideal state if at all possible. We adopt this second definition of absolute stability in both sediment flux and sandbar form as an analytical standard (though not necessarily as an expected operational reality) for this study. Since one of the major management concerns facing Grand Canyon National Park is limited sediment supply, this stricter minimal-flux stability concept is, in essence, the desired operational target.

### Study Objectives

One of the early observations noted by GCES researchers during the Test Flows was a substantial change in sandbar morphology that occurred over surprisingly short time intervals. Visual observations included active sandbar face calving and oversteepened sandbar faces. Volumetric survey data also indicated that major changes in sandbar morphology occurred between field survey visits. One early method for monitoring sandbar morphology consisted of placing thin wire cables (erosion chains) of known length vertically into sandbars at node points of precisely surveyed grids. In theory, the wires could be remeasured twice monthly. In actuality, follow-up surveys could not even relocate large portions of the wire grids.

From these casual observations, it is apparent that the sampling interval of most sediment studies was not short enough to capture all processes affecting sandbar morphology in the Grand Canyon (Howard and Dolan 1979; Schmidt and Graf 1990; Beus 1992). Thus, this project had two major objectives: (1) development of methods to investigate short-term changes in sandbar morphology; and (2) interpretation of sandbar stability and longevity as distilled from these methods.

We hypothesize that substantial changes in sandbar morphology, and associated exchange of sediment to subaqueous locations, are occurring routinely at time scales as short as a few hours, and that these escaped detailed analysis in the Test Flow studies. Such rapid change, while not surprising in many geomorphic settings, has not been documented quantitatively, or even described, in previous Grand Canyon sediment research. If such sudden changes in sandbar morphology occur, they are most likely affecting sandbar longevity, and they need to be accounted for in any sediment resource-management plan. Further, the characteristics of these short-term sandbar processes will affect assumptions of substrate stability that impact the behavior of other components of the riverine ecosystem. While some geomorphologists may be comfortable with a form-based equilibrium definition of sandbar stability, an ecologist studying vegetation patterns on sandbar substrate may find the cycling sediment in such a system to be far from a "stable" substrate for vegetation.

## Methods

To detect and quantify short-term change in sandbar morphology, we devised a time-lapse repeat photography technique. The overall experimental design involved three specific tasks: (1) establish a daily photographic record of sandbar stability along the Colorado River between Lees Ferry and Diamond Creek, (2) digitalize and rectify selected images from a subset of these sandbars for further analysis, and (3) analyze the temporal and spatial changes in sandbar size and morphology at time steps measured in hours to days.

### Site Selection and Description

We selected twenty-one of the forty-three sandbars monitored at various times over the five-year study (Figure 2) for change detection in this paper. We chose these sites because they are distributed throughout all major geomorphic reaches in Grand Canyon (Schmidt and Graf 1990) and because they had the best temporal fidelity. Field descriptions of each rectification site are listed in Table 1. By convention, locations throughout the Colorado River corridor are designated by "river mile," referenced to downstream travel from Lees Ferry (Stevens 1991). We analyzed images obtained daily over 1170 days between March 1992 and May 1995. A 120-day gap in the record during the summer of 1994 coincides with a period for which no funding was available to service the cameras.

## Field Methods

Land-based, high-oblique, single-camera-position photogrammetry was employed (Cluer 1992; Cluer and Dexter 1994; Dexter and Cluer 1996). These time-lapse camera systems were built from inexpensive, off-the-shelf products (about $200 per site plus recovery and processing costs) consisting of Pentax IQZ 105 programmable cameras. The microprocessor-controlled cameras can be set for repeat exposures once every twenty-four hours. Each camera was secured to an alignment base sized to fit snugly inside a military ammunition can. A large round hole was cut into the side of the can, congruent with the position of the camera lens, and fitted with a Plexiglas window. A small metal gable was attached to protect the Plexiglas from the elements. The boxes were painted in earth-tone colors to render them inconspicuous to park visitors.

At each site, a single camera was positioned at a sufficient distance to photograph the entire sandbar. Cameras were typically located across the river, high on the talus slopes, to provide a high-oblique view of the sandbar (for example, see Figure 7). Camera boxes were attached to large boulders or to bedrock outcrops with silicon sealant. Timers were set to expose the film daily at a predetermined time to take advantage of local low river stage and to avoid shading effects. Each camera was loaded with thirty-six-exposure, color slide film (color negative film has been used since January 1995), and sealed in the box along with a packet of desiccant. Control panels, of the type used in conventional aerial photography, were temporarily fixed at points on the sandbar within the field of view (Figure 7). Coordinates of the panels and of the camera lens/film plane were measured using a total-station and standard plane-surveying techniques. After the first exposure, the control panels were removed. Film was recovered and replaced on a monthly basis.

## Image Processing

Initially, the film was processed conventionally and left in strips to facilitate scanning. A high-resolution Nikon LS-3510AF film scanner was used to convert the analog images to digital form. The digital Tagged Image Format (TIF) file created by the scanner was manipulated using Picture Publisher software. Beginning in January 1995, film processing included transfer to CD-ROM. Digital images were imported into ERDAS V.7.5 and Imagine V.8.2 for image rectification and analysis (ERDAS 1992). Figure 8 shows the sequence of steps involved in the entire process.

**Table 1.** Description of Twenty-One Sandbars Studied

| River Mile | Name/Description | Type | Time of Low Water |
|---|---|---|---|
| 2.6 L | Above Cathedral Wash | Reattachment | 7-10 am |
| 16.4 L | Hot Na Na Camp | Eddy | 10 am-1 pm |
| 43.1 L | Anasazi Bridge Camp | Upper pool | 3-6 pm |
| 44.6 L | Eminence Break | Separation | 3-6 pm |
| 44.65 L | Eminence Break | Reattachment | 3-6 pm |
| 60.1 R | Large bar on right below 60 mile | Eddy | 4-7 pm |
| 61.8 R | First bar below LCR on right | Separation | 4-7 pm |
| 64.0 L | Hopi Salt Mines | Reattachment | 4-7 pm |
| 81.2 L | Grapevine Camp | Channel margin | 5-8 pm |
| 119.0 R | 119 Mile Creek Camp | Reattachment | 7-10 am |
| 122.3 R | 122 Mile Creek Camp | Reattachment | 8-11 am |
| 122.7 L | Upper Foster Canyon Camp | Upper pool | 8-11 am |
| 132.0 R | Below Stone Creek Camp | Reattachment | 9 am-12 pm |
| 136.6 L | Pancho's Kitchen | Separation | 9 am-12 pm |
| 136.7 L | Pancho's Kitchen | Reattachment | 9 am-12 pm |
| 145.5 L | Abve Olo Canyon Camp | Reattachment | 10 am-1 pm |
| 172.2 L | Below Mohawk Canyon | Separation | 3-6 pm |
| 172.3 L | Below Mohawk Canyon | Reattachment | 3-6 pm |
| 173.1 L | Camp below riffle at 173 mile | Eddy | 3-6 pm |
| 211.3 L | Above Fall Canyon | Eddy | 4-7 pm |
| 212.9 L | Pumpkin Spring Camp | Upper pool | 4-7 pm |

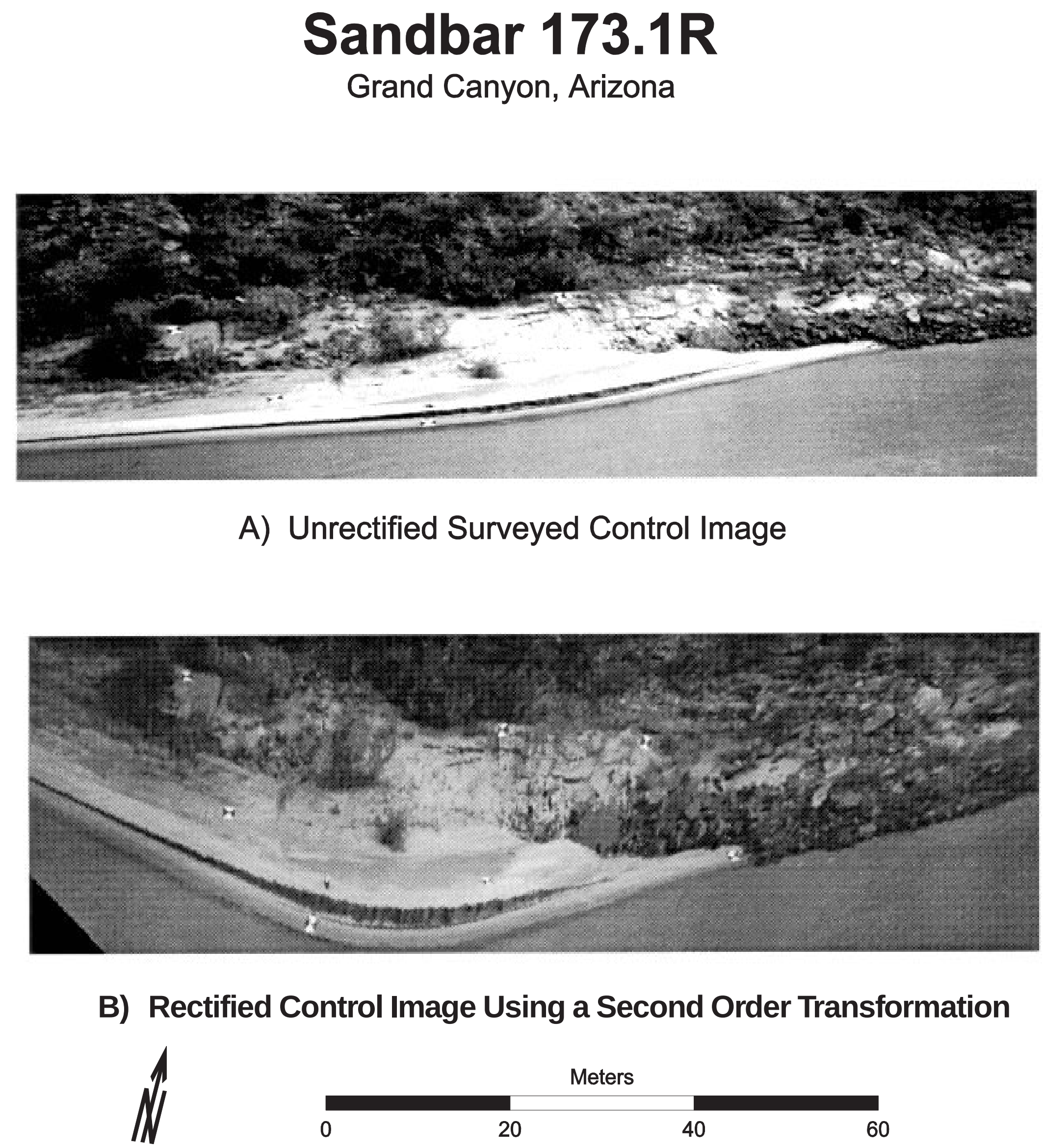


**Figure 7.** Examples of an oblique image (a) and a matching rectified image (b) showing control panels in place.

Selected images were rectified from an oblique view to a planimetric model to facilitate sandbar area measurements (Figure 7). Pixel coordinates of the control panels in the digital images were matched with real-world coordinates on the ground, using a variety of transformation equations (ERDAS 1992). Higher-order equations are beneficial in reducing error between image and ground coordinates, but required a larger number of ground control points. Once an optimal transformation equation was established, control panels became redundant because fixed natural features in the images can be used to control subsequent transformations. Following transformation, the image becomes a planimetric model of the sandbar with all pixels referenced to real-world units (meters).

Some images were difficult to rectify due to poor photographic exposure (e.g., from poor sun angle or shadowing from steep cliffs). Fortunately, digital images can be separated into the three primary colors (red, green, and blue) and these

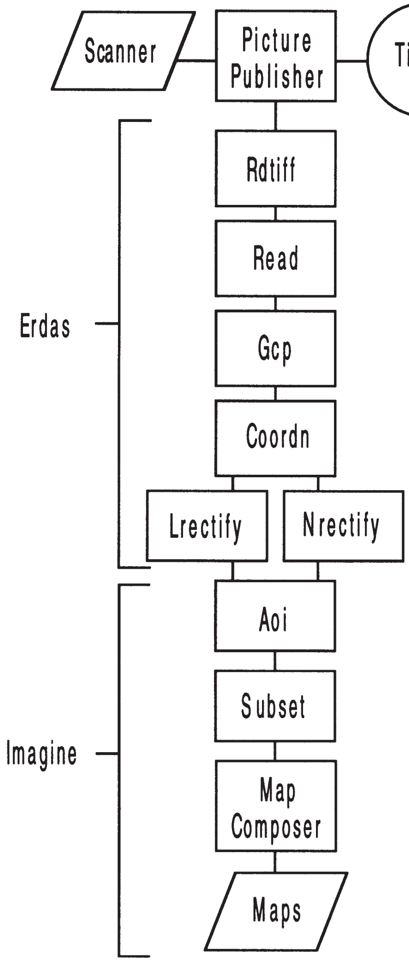


**Figure 8.** Flow chart showing the ERDAS and IMAGINE software modules used in this study.

spectral bandwidths can be analyzed individually. By manipulating the saturation of each color in ERDAS, various details could be enhanced. For example, increasing the amount of blue enhances information in dark shadows. Decreasing the red can enhance features washed out by overexposure. This procedure allowed us to customize each image, bringing out useful detail that would have been unseen otherwise.

After image rectification, the planimetric photo models were screen-digitalized using the area-of-interest (AOI) module in Imagine V.8.2 to obtain area and perimeter measurements. Lateral erosion or deposition was established by comparing planimetric image pairs. It is essential to appreciate that quantitative estimates of sandbar topography and volume cannot be made with these methods, and that this is a methodological constraint. The AOI module also produced digital polygon files that enabled the rectified image of each sandbar to be extracted and placed into a map composition using Imagine SUBSET and MAP COMPOSER modules, respectively, to produce imaged maps of the sandbars (e.g., Figures 9, 10).

We made error estimates using total-station surveys of several key point locations and comparing the equivalent locations to the rectified images. In addition, we performed a more structured error analysis, using photos taken from a high-rise building with carefully surveyed points and areas marked on parking lots adjacent to the building. Results from both types of error analyses indicate a +/– 1 meter point position accuracy at the 95-percent confidence level, and +/– 2 percent area error when applied to the sandbar images used in this study. Methodological problems associated with this technique include extreme high-oblique rectification, some topographic relief problems, visual estimation error between analysts, and day-to-day variation in river stage. Stage-change problems were minimal due to the close temporal proximity of the images used. In general, this application of the methodology presented the fewest problems and the analytical error approached the above stated procedural confidence intervals.

## Analytical Procedures

Raw oblique photographs were inspected visually to identify significant changes in each sandbar and their relative timing. Once we detected an erosional "event," we rectified and compared the images preceding and following the event to estimate the area change during it. Rapid failure of sandbars was readily documented (Figures 11a, b, and c) and quantified (Figures 9, 10). The fine temporal resolution of spatial processes was the most significant benefit of the technique.

We used similar imaging techniques in long-term monitoring (usually monthly time-steps) and in rectifying those images to estimate sandbar area. Cameras were set to expose at local low water in order to correlate sandbar area with minimum discharge. Based on the expected three-day kinematic wave residence time through Grand Canyon, three-day-moving-means of minimum dam discharge were used to estimate river flow at the time of the photographs.

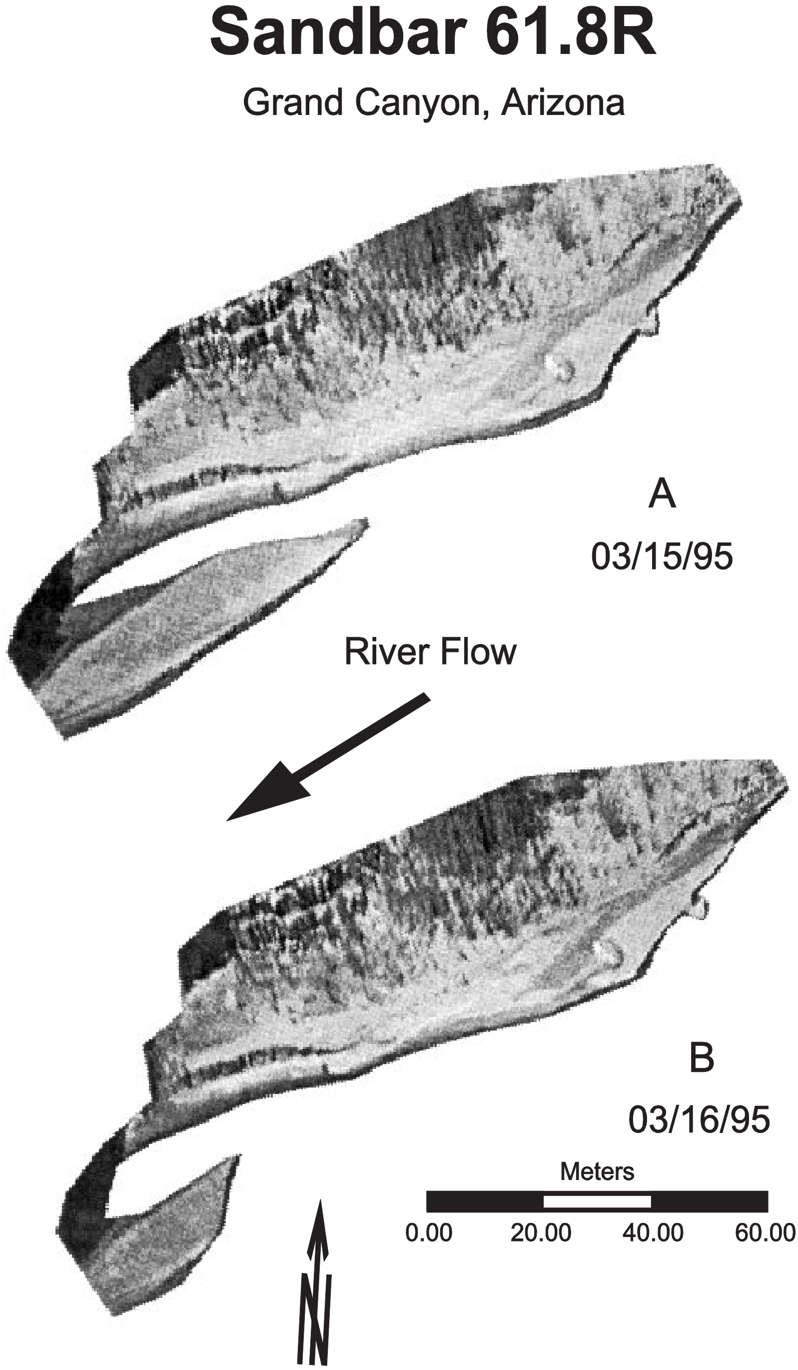


**Figure 9.** Examples of two rectified images for sandbar 61.8R showing sandbar area loss between March 15, 1995 (top) and March 16, 1995 (bottom). Note the sharp cutbank formed on the eddy bar and the associated loss of 609 $m^2$ of sandbar area shown in the bottom image.

The basic analytical approach was to compare sandbar area distribution statistics and sandbar area values in time-series mode. The mean, standard deviation, skewness, and kurtosis values for the area of each sandbar were derived along with raw area-frequency histograms. Extension of this

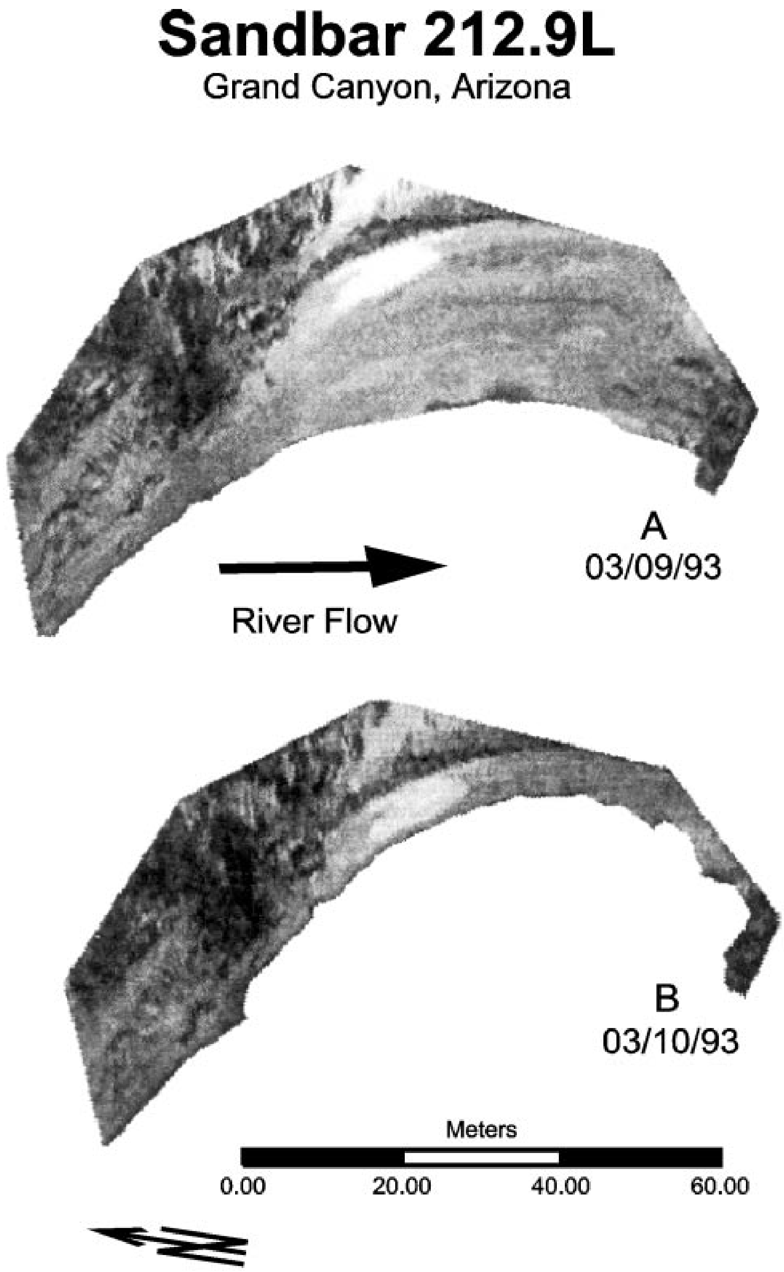


**Figure 10.** Examples of two rectified images for sandbar 212.9L showing 936 $m^2$ sandbar area loss between March 9, 1993 (top) and March 10, 1993 (bottom).

basic methodology to longer-term monitoring posed additional analytical problems. Such problems included estimating the morphology expected from stable sandbars, determining the effect of a slightly nonnormal maximum and minimum discharge distribution, and determining the effect of change in subaerial extent of exposed sand with change in river stage.

**Figure 11a.** High oblique image of sandbar 16.4 L, acquired (a) on October 22, 1992, before rapid failure.

**Figure 11b.** High oblique image of sandbar 16.4 L, acquired (b) on October 23, 1992, during rapid failure.

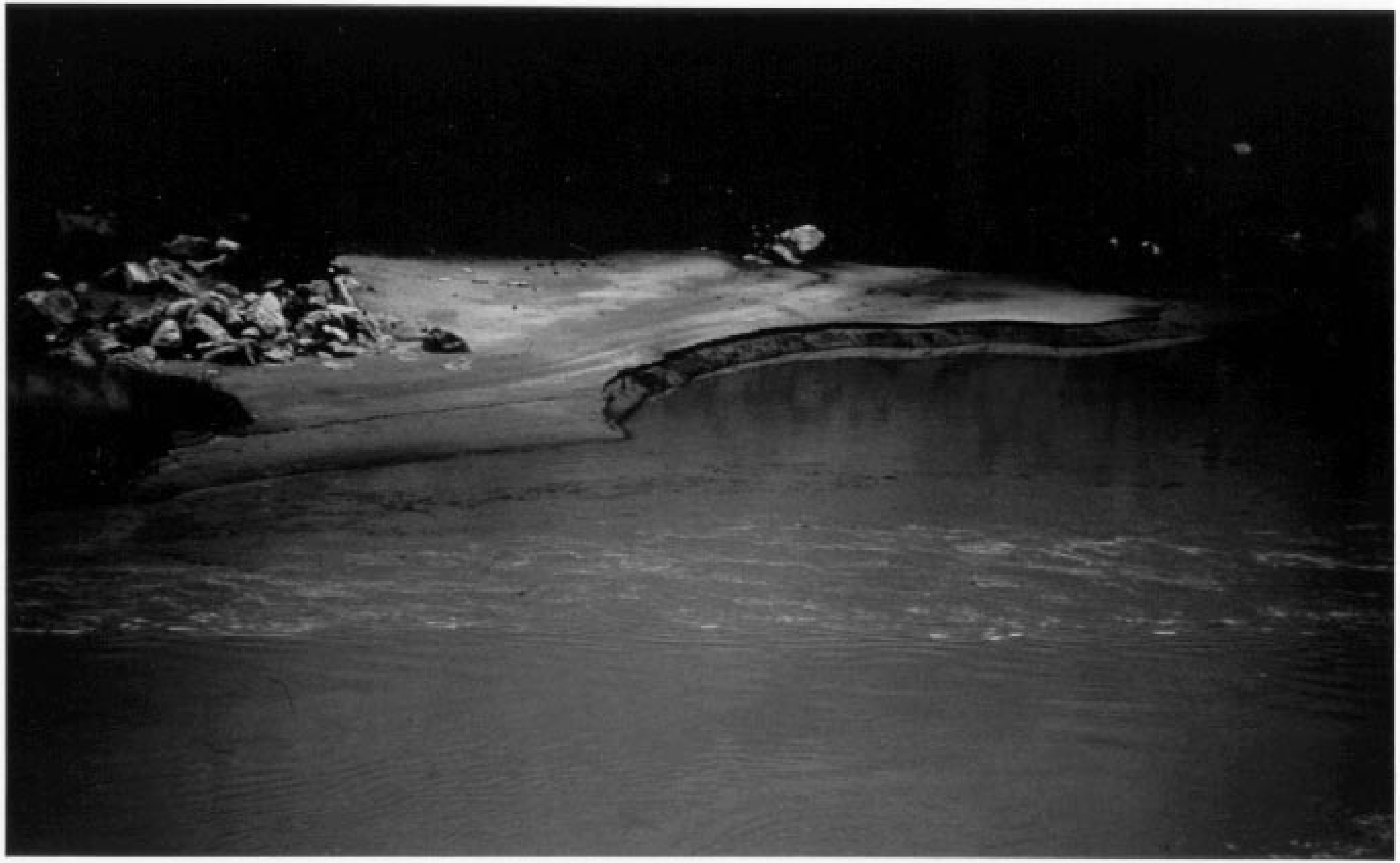

**Figure 11c.** High oblique image of sandbar 16.4 L, acquired (c) on October 24, 1992, following rapid failure.

## Development of Comparison Controls and Mitigation of Analytical Problems

Since all sandbars in the study area are subject to morphological change, there is no natural control or baseline sandbar against which we can evaluate stability. A numerical, synthetic, control sandbar that remains constant over the study was therefore established (Figure 12). The "shape" of this fixed synthetic sandbar was selected to approximate the hypsometry of a typical Grand Canyon sandbar between the maximum and minimum discharge values of the Interim Flow Prescription (the "fluctuating zone" in Figure 3). In addition, we assumed a reasonably accentuated S-shaped profile to propagate worst-case error through the analysis. Most real sandbars have more linear hypsometric curves under conditions of the Interim Flow Prescription (Kaplinski et al. 1996); thus our area-change interpretations are conservative. By tracking the subaerial area of the synthetic sandbar left exposed during fluctuating discharge conditions, expectations for the variability in area measurements due to stage changes alone could be established. If departures were found to lie beyond those of the synthetic sandbar (Figure 12), these departures can be taken as a signature of change, and thus instability.

We discovered that extreme high and low dam discharges tended to be slightly bimodal in distribution, as opposed to the near-normal distribution of mean flows (Figure 5a). Since we were also detecting pronounced bimodality in sandbar area measurements, we wanted to be sure the area changes were stability-related and not discharge-related. In order to assess the effects of nonnormal discharge patterns on sandbar area calculations, we separated the sandbar area dataset into two parts around a minimum flow of 240 cms (8,500 cfs) and analyzed each part separately. If partitioned results compare with the full dataset results, then flow bimodality is most likely not responsible for bimodality in area measurements. Based on this test, it is our opinion that the bimodal area distribution is not directly produced by the slightly bimodal distribution of the extreme flows.

Poorly defined stage-to-discharge relationships presented another problem. Localized reworking of bed deposits over time can alter channel geometry that, in turn, alters the stage-to-discharge relationship. This problem has not been fully solved. We used data from survey-based

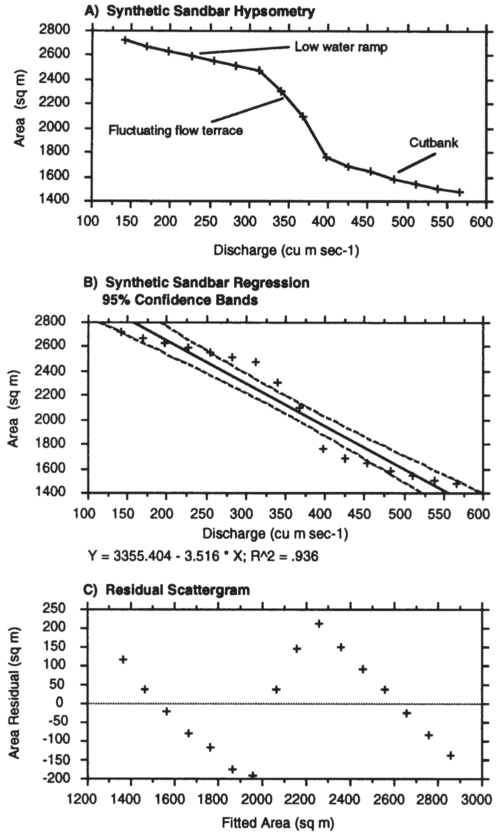


**Figure 12.** Characteristics of the synthetic control sandbar. The top panel (a) shows the discharge hypsometry, the middle panel (b) shows the area versus discharge regression, and the bottom panel (c) shows the regression residuals. Note the serial correlation in the residuals resulting from the unchanging shape.

studies and statistical methods to help remove the effect of river stage conditions over long time intervals. Other sandbar erosion projects have been executed contemporaneous with the photogrammetry work discussed here. Kaplinski et al. have conducted area and volume surveys of thirty sandbars about twice a year since 1991. They use total-station surveying and bathymetric sounding techniques to develop surface models of each sandbar. The advantage of the Kaplinski dataset is that the changing-stage versus exposed-sandbar volume problem has been removed. Work by Kaplinski et al. (1996) showed a nearly linear relation between stage and discharge at thirty sandbars. If we constrain these relations to flows below 567 cms (20,000 cfs), the upper limit of the Interim Flow Prescription, a linear approximation of stage discharge is very reasonable ($R^2$ greater than 0.95). We adopted the near-linear stage-discharge relations developed and tested by Kaplinski et al. (1996). Of the twenty-one sandbars we monitored, eleven were the same as those studied by Kaplinski et al.

The most useful error-correction method incorporated regression and residual analyses (Figures 13 and 14) on the sandbar area versus discharge relationships. Since sandbar area fluctuates with discharge (lower discharge exposes more of the sandbar), we would expect a strong negative correlation between the two variables. We should be able to improve our area estimates by removing the regression trend (which mostly represents average stage-area effects). Next, we discount residuals lying within the 90 percent confidence interval of the regression line (which mostly represents localized shape-hypsometry variability). Finally, we analyze the remaining extreme residuals (which mostly represent substantial area change). A stable sandbar will also impart another telltale fingerprint. Stable geometry will lead to a very distinct pattern of serial correlation within the area residual scatter accrued during fluctuating discharge. This effect is clearly illustrated in the results from the synthetic control sandbar (Figure 12).

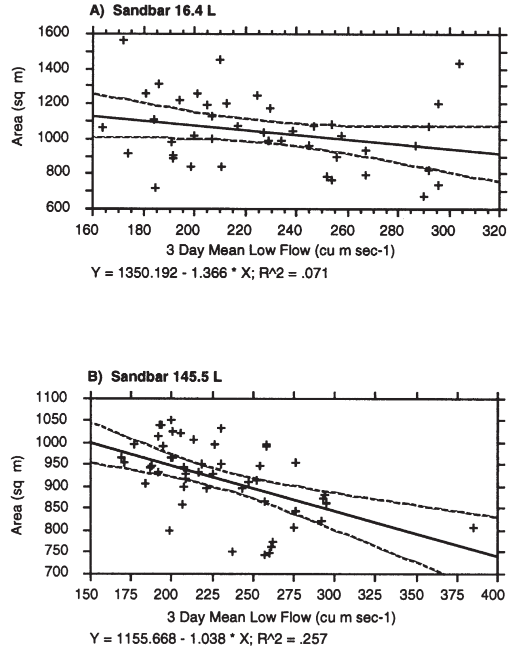


**Figure 13.** Example regression plots for sandbar area versus three-day average minimum discharge from two selected sandbars (16.4L and 145.5L) typical of the twenty-one sandbars included in this study.

## Results

### Sandbar Instability at Daily Temporal Resolution

Over the five years of study, nearly 100 rapid-failure events were photographed. Fifty-two of these were selected for further analysis, and they occurred on fourteen of the twenty-one study sandbars. Thus, only seven sandbars displayed no rapid-failure events. Sandbar areas involved in rapid failure ranged from 9 m$^2$ (representing 1 percent of the total area) to 936 m$^2$ (representing 52 percent of the total bar area). The modal value of failure area was 5–7 percent of the total bar area. The greatest daily lateral retreat captured in the photographs was 40 m at eddy bar 61.8R on March 15-16, 1995 (Figure 9). More typically, daily lateral retreat during failure events was approximately 20 m (Figure 10). Lateral erosion rates of retreating sandbar faces captured in this study are two orders of magnitude larger than previously reported (Table 2, Figure 15) (Howard and Dolan 1979; Beus 1992; Schmidt and Graf 1990). A feeling for the dynamics of such rapid-failure events can be gained by studying some details of the very active eddy/reattachment bar at 172.3L. The common pattern begins with the rapid-failure event itself, where a substantial portion of the bar is lost to erosion in as little as a few hours. Following failure, redeposition fills in the eddy zone over a period of a few weeks until the deposit reaches an elevation where it is consistently exposed at daily low stage. Deposition rates decrease and the physical size of the eddy bar remains relatively stable at a maximum size for a prolonged period of time. Rapid-failure erosion of the eddy/reattachment deposit occurs again, reducing sandbar area to a minimum, and the cycle repeats.

This failure sequence has been directly observed in the field on two significant occasions. The first occurred April 17, 1991, during rising stage. The initial indication of erosion was the formation of short (.25 m) vertical cutbanks along the river-proximal edge of the sandbar. Parallel fractures appeared in the bar surface about 0.5 to 1.5m back from the cutbank. Subsequently, blocks of cohesive sand rotated toward the river as their bases were eroded at water level. This

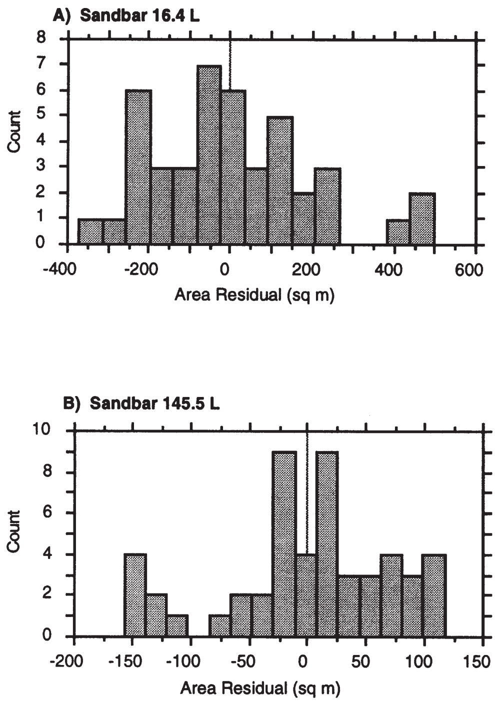


**Figure 14.** Example frequency histograms for residuals of sandbar area versus three-day average minimum discharge for regressions from two selected sandbars (16.4L and 145.5L) typical of the twenty-one sandbars included in this study.

process advanced into the eddy bar, entirely eroding it along with portions of the adjacent vegetated reattachment bar. The well-established riparian vegetation provided little discernible stabilizing influence. Erosion was most active 1–2 m below the deposit surface, where mostly taproots existed. The entire eddy bar was eroded in less than four hours and the bank retreat rate was so rapid that it was disconcerting to make measurements or observations close to the active edge. The area involved in the event was about 250 m$^2$. The volume eroded during the event was estimated at 5,000 m$^3$ by soundings conducted on April 18.

A second event occurred in July 1993 that included both the separation bar (172.2L) and the eddy-reattachment bar (172.3L). At noon on July 25, during daily low stage, a semicircular area on the downstream face of the separation bar began eroding. The driving mechanism appeared to be a secondary flow vortex in the recirculation zone with sufficient spatial and temporal permanence to scour sand from submerged as well as subaerial portions of the deposit. The vortex persisted for about three hours and eroded an area about 50 m$^2$ with an estimated volume of 50 m$^3$. Erosion ceased as daily stage increased, and no additional erosion was observed. During the following discharge cycle, approximately 0.15 m of sand was evenly deposited over the top of the eddy bar. An additional 0.05 m of sand was deposited on top of the eddy bar during high stage on July 26. As stage increased on July 27, about 8:30 p.m., failure initiated along the river-proximal side of the eddy bar in a fashion much like that observed on April 17, 1991. Within about three hours, the eddy deposit was completely eroded by high-velocity currents and retreat of the bank along vertical faces.

The timing of these events suggests a definite process linkage between the sandbar types that reside within one riffle-pool unit. On four occasions, failure of the separation bar preceded failure of the eddy bar by two days, while on another occasion, the lag was only one day. Pre- and post-event topographic and bathymetric surveys were conducted, yielding a volume loss of 12,000 m$^3$ from an eroded surface area of 450 m$^2$. Events with similar area losses were documented ten times at 172.3L between March 1992 and October 1995. If one assumes that surface area change corresponds roughly to the volume of material eroded, the ten events documented at 172.3L represent approximately 80,000 m$^3$ of sediment exchange between the channel and channel-margin storage over thirty-eight months. A conservative estimate of the monthly average is approximately 2,100 m$^3$. This corresponds to a minimum of 33,000 metric-ton exchanges on an annual basis at one sandbar only. Volume exchanges during some known events were not measured, and an unknown number of additional events likely occurred during breaks in the record.

## Long-Term Sandbar Instability

During the study, all sandbars experienced changes in surface area with frequent increases and decreases around a modal value (Figure 16). No sandbar had a minimum area configuration at the end of the study period suggesting that continuous erosion is not the norm. The largest change occurred at 2.6L with a relative difference of 78 percent, whereas the smallest change occurred at 81.2L with a relative difference of 19 percent. One of the best comparative indicators

**Table 2.** Summary of Measured Lateral Erosion and Deposition Rates with Sampling Frequency from Several Studies

| Reference | Sample Interval (days) | Maximum Reported Erosion Rate[a] m day-1 | Maximum Reported Erosion Rate[a] m year-1 | Maximum Reported Deposition Rate m day-1 | Maximum Reported Deposition Rate m year-1 |
|---|---|---|---|---|---|
| Beus (1992) | 3652 | 0.002 | 0.8 | 0.005 | 1.7 |
| Howard & Dolan (1979) | 2922 | 0.003 | 1.15 | 0.002 | 0.7 |
| Howard & Dolan (1979) | 365 | 0.007 | 2.45 | 0.002 | 0.7 |
| Schmidt & Graf (1990) | 135 | 0.100 | 34.7 | 0.073 | 26.7 |
| Beus et al. (1992) | 14 | 1.42 | 520 | 1.069 | 390 |
| This study | 1 | 20-40 | 7315-14629 | 7.0 | 2550 |

[a]The values in this table should be used as indicators of sediment cycling activity rather than as a measure of any accumulated effect directly observable in the environment over the reported time-step.

of sandbar activity is the coefficient of variation (standard deviation divided by mean area), because the effect of deposit size is removed. Sandbar 60.1L had the largest CV (0.33) for the study, reflecting the sensitivity of its position immediately downstream from the confluence of the Little Colorado River. Sandbar 81.2L displayed the smallest CV (0.049), reflecting its rock-bound siting which provides an unusual amount of protection.

Frequency distributions of area measurements for each sandbar are consistently nonnormal and usually tail-heavy (Table 3, Figure 14). Such nonnormality is not consistent with expectations for stable simple-geometry sandbars. Nevertheless, the possibility of stable sandbars with complex nonlinear hypsometry is not precluded, even though complex hypsometry is rare in Grand Canyon sandbars. The bimodal area distributions persist even at subseasonal time partitions, which is a further indication that sandbar area distributions are not necessarily bimodal as a function of simple area exposed during seasonal discharge levels. Most regression analyses indicate a significant, negatively correlated stage-area relationship that can be attributed to variations in discharge alone. This correlation is manifested as the slope of the regression line and the persistence of serial correlation in the residuals. It is interesting to note that the strength of the stage-to-area relationship decreases downstream. Three sandbars return a positive correlation, but the large residual scatter renders the regressions not statistically significant.

It is noteworthy that the regression analyses of the real sandbars (Figure 13) yield large scatter well beyond that expected by stage variation alone (beyond the 90 percent confidence interval of the regression line), when compared to results for the synthetic stable sandbar. Such scatter, we contend, is indicative of unstable area configurations, because the scatter contains no serial correlation that would be expected for a stable sandbar (Figure 12). It is possible that sandbars could be dynamically changing shape without net volume change and vice versa. Our methods are not able to discriminate such processes, but total-station surveys by Kaplinski et al. (1996) suggest that they do occur at coarser time steps. Frequency distribution of the residuals is typically nonnormal and bimodal (Figure 14), but low-flow bimodality does not appear to have a significant effect on area distributions. Time-series of area residuals display some persistent patterns (Figure 16), wherein sandbar area remains relatively consistent through time until some rapid "event" occurs that changes the area drastically. Area loss is often associated with low flow during or shortly after a weekend. Area loss can also be associated with a continuous drop in flow over several days as the seasonal flow regime changes.

## Discussion

### Operation of Glen Canyon Dam during the Study

Figure 4 presents time-series plots of daily discharge and accumulated seven-day change in discharge. Figure 5 shows a frequency histogram and correlogram of daily mean discharge at Glen Canyon Dam for all study days. The mean flow is nearly normal in distribution. Note the pronounced seven-day lag-positive peak and successive seven-day harmonic-positive peaks (Figure 5a)

**Table 3.** Summary of Long-Term Change for Sandbars in Study

| Sandbar | Begin Area ($m^2$) | End Area ($m^2$) | Area Change (%) | Maximum Area ($m^2$) | Minimum Area ($m^2$) | Total Difference (%) | Mean Area ($m^2$) | Standard Deviation | Coefficient of Variation | Skewness | Kurtosis |
|---|---|---|---|---|---|---|---|---|---|---|---|
| 2.6 L | 1529 | 2101 | 37.41 | 2885 | 633 | 78.06 | 1788 | 566 | 0.318 | 0.28 | –0.64 |
| 16.4 L | 1064 | 0955 | –10.24 | 1565 | 676 | 56.81 | 1038 | 202 | 0.195 | 0.46 | –0.09 |
| 43.1 L | 2946 | 2795 | –5.13 | 3121 | 2376 | 23,87 | 2740 | 192 | 0.070 | –0.08 | –1.01 |
| 44.6 L | 876 | 0573 | –34.59 | 898 | 347 | 61.36 | 628 | 132 | 0.209 | –0.03 | –0.38 |
| 44.65 L | 5288 | 3890 | –26.44 | 5733 | 2194 | 61.73 | 3996 | 934 | 0.234 | 0.03 | –1.03 |
| 60.1 R | 0809 | 1824 | 125.46 | 2460 | 620 | 74.80 | 1635 | 538 | 0.330 | –0.45 | –0.90 |
| 61.8 R | 3247 | 4322 | 33.11 | 5487 | 2331 | 57.52 | 4134 | 730 | 0.177 | –0.39 | –0.34 |
| 64.0 L | 3277 | 3921 | 19.65 | 5662 | 1850 | 67.33 | 3327 | 894 | 0.269 | 0.82 | 0.55 |
| 81.2 L | 1896 | 1932 | 1.90 | 1987 | 1611 | 18.92 | 1853 | 91 | 0.049 | –1.00 | 0.34 |
| 119.0 R | 3953 | 4351 | 10.07 | 4365 | 2811 | 35.60 | 3925 | 331 | 0.084 | –1.16 | 1.15 |
| 122.3 L * | 5429 | 4243 | –21.85 | 5429 | 3261 | 39.93 | 4331 | 609 | 0.141 | –0.18 | –0.87 |
| 122.7 L | 3162 | 3321 | 5.03 | 4149 | 2297 | 44.64 | 3354 | 371 | 0.110 | –0.18 | 0.50 |
| 132.0 R * | 2233 | 2738 | 22.62 | 3140 | 2233 | 28.89 | 2744 | 271 | 0.099 | –0.57 | –0.83 |
| 136.6 L * | 1220 | 1152 | –5.57 | 1347 | 843 | 37.42 | 1192 | 120 | 0.101 | –1.28 | 1.54 |
| 136.7 L * | 2861 | 2025 | –29.22 | 3196 | 2025 | 36.64 | 2664 | 283 | 0.106 | –0.40 | 0.63 |
| 145.5 L | 907 | 998 | 10.03 | 1051 | 745 | 29.12 | 918 | 85 | 0.092 | –0.47 | –0.68 |
| 172.2 L | 770 | 596 | –22.60 | 851 | 504 | 40.78 | 673 | 98 | 0.146 | –0.19 | –1.11 |
| 172.3 L | 1549 | 1447 | –6.58 | 2263 | 1024 | 54.75 | 1710 | 280 | 0.164 | –0.07 | –0.38 |
| 173.1 L | 1433 | 1560 | 8.86 | 1977 | 1251 | 36.72 | 1548 | 187 | 0.121 | 0.17 | –0.89 |
| 211.3 L | 4013 | 3629 | –9.57 | 4839 | 3045 | 37.07 | 3825 | 453 | 0.119 | 0.42 | –0.44 |
| 212.9 L * | 2249 | 2070 | –7.96 | 2911 | 1442 | 50.46 | 2145 | 442 | 0.206 | –0.15 | –1.11 |
| Mean | 2415 | 2402 | 4 | 3110 | 1625 | 46 | 2389 | 372 | 0.159 | –0.21 | –0.29 |
| Std. Dev. | 1427 | 1280 | 34 | 1637 | 901 | 16 | 1222 | 258 | 0.079 | 0.52 | 0.78 |

*Indicates length of record shorter than 1170 days.

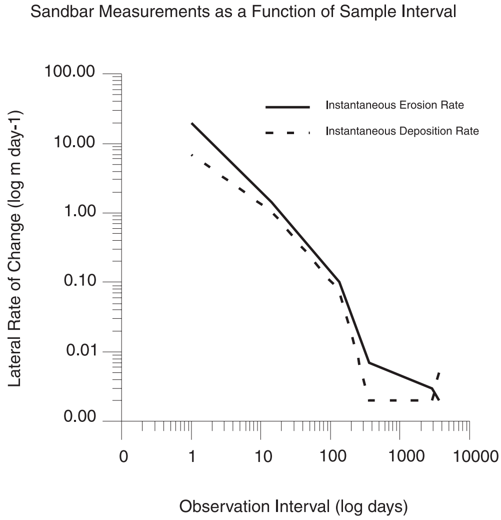


**Figure 15.** Log-scaled plot of measured lateral erosion rates versus sample frequency, using data from several Grand Canyon sediment studies. This plot summarizes the data in Table 4.

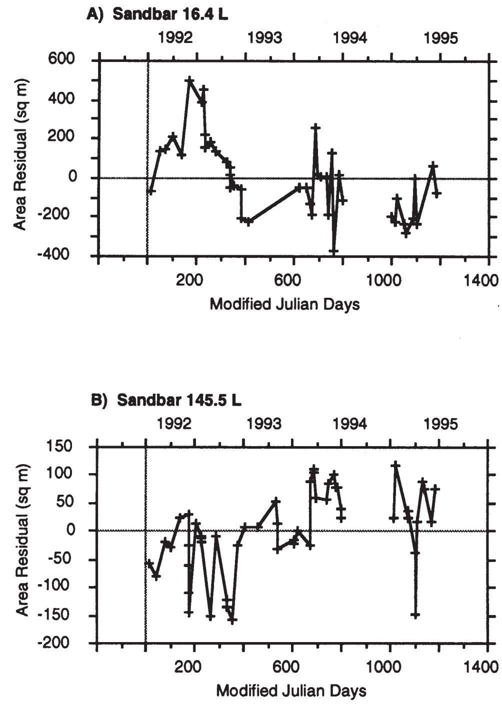


**Figure 16.** Example time-series plots for residuals of sandbar area versus three-day average minimum discharge for regressions from two selected sandbars (16.4L and 145.5L) typical of the twenty-one sandbars included in this study. Modified Julian day number one is March 1, 1992.

produced by consistent weekend low flows. Discharge is also subject to periods of accumulated multiday increases or decreases (Figure 4b). Neither of these flow characteristics are directly addressed in the Interim Flow Prescription, and both may prove significant in continued sediment cycling and sandbar reworking, as we discuss later (also see Cluer et al. 1993). The frequency distribution analysis of mean discharge for photo days only is similar, suggesting we have area estimates from a representative set of flow conditions.

## Modes of Sandbar Failure

This study has shown that rapid failure events occur commonly on Grand Canyon sandbars (Figures 11a, 11b, and 11c). Sediment exchange of this type and rate has not been documented in previous Grand Canyon sediment studies (Table 2, Figure 15). Sandbar erosion appears to proceed in two modes. The first is a "gradual" mode where small quantities of sediment erode over time scales of days to weeks. The second is an "event" mode as revealed in this study. In this case, failure of the sandbar along the channel-proximal edge moves significant amounts of sediment from subaerial storage to subaqueous storage in eddies or to the main channel where it is transported downstream. These events occur over time scales as short as a few hours and appear to display very large instantaneous lateral erosion rates.

The common pattern begins with the rapid-failure event itself, where a substantial portion of the bar is lost to erosion in as little as a few hours. Following failure, redeposition fills in the eddy zone over a period of a few weeks until the deposit reaches an elevation where it is consistently exposed at daily low stage. Deposition rates decrease, and the physical size of the eddy bar remains relatively stable at a maximum size for a prolonged period of time. Rapid-failure erosion of the eddy/reattachment deposit occurs again, reducing sandbar area to a minimum, and the cycle repeats.

Most rapid-failure events occur in conjunction with sudden or prolonged periods of discharge reduction. Such discharge reduction occurs commonly in the form of weekend low flows or as between-season, multiday reductions in flow riffle units. The exact combination of factors favoring rapid failure over longer-term erosion,

**Table 4.** Summary of Rapid-Erosion Events for Twenty-One Sandbars Studied

| Sandbar | 2.6L | 16.4L | 43.1L | 44.6L | 44.65L | 60.1R | 61.8R | 64.0L | 81.2L | 119.0R | 122.3R |
|---|---|---|---|---|---|---|---|---|---|---|---|
| Mean area ($m^2$) | 1788 | 1038 | 2740 | 628 | 3996 | 1635 | 4134 | 3327 | 1853 | 3925 | 4331 |
| Area lost ($m^2$) 1992 | 924(6) | 56(1) | 82(1) | | 201(6) | | 36(0) | 400(0) | | | |
| | | | 35(5) | | | | 28(0) | | | | |
| | | | 53(1) | | | | | | | | |
| Area lost ($m^2$) 1993 | 473(1) | 104(0) | | | | | 71(0) | 552(5) | | 235(0) | 396(0) |
| | | 30(0) | | | | | | | | 91(3) | |
| | | | | | | | | | | 113(0) | |
| Area lost ($m^2$) 1994 | | | | | | | | | | | N.D. |
| Area lost ($m^2$) 1995 | | | 14(2) | | | | 609(3) | | | | N.D. |
| | | | | | | | 720(2) | | | | |
| N | 2 | 3 | 4 | 0 | 1 | 0 | 5 | 2 | 0 | 3 | 1 |
| Sum | 1397 | 190 | 184 | 0 | 201 | 0 | 1464 | 952 | 0 | 439 | 396 |
| Mean | 699 | 63 | 46 | 0 | 201 | 0 | 293 | 476 | 0 | 146 | 396 |
| Standard deviation | 319 | 38 | 29 | 0 | | 0 | 342 | 107 | 0 | 78 | 0 |
| Return interval | 585 | 390 | 293 | 0 | 1170 | 0 | 234 | 585 | 0 | 390 | 640 |

| Sandbar | 122.7L | 132.0R | 136.6L | 136.7L | 145.5L | 172.2L | 172.3L | 173.1R | 211.3L | 212.9L |
|---|---|---|---|---|---|---|---|---|---|---|
| Mean area ($m^2$) | 3354 | 2744 | 1192 | 2664 | 918 | 673 | 1710 | 1548 | 3825 | 2145 |
| Area lost ($m^2$) 1992 | | N.D. | | | 137(0) | 5(0) | 214(3) | | | |
| | | | | | 3(0) | 21(4) | 118(2) | | | |
| | | | | | | 6(1) | 533(0) | | | |
| Area lost ($m^2$) 1993 | 44(3) | N.D. | | | 13(0) | 75(0) | 199(1) | | 242(3) | 936(1) |
| | | | | | 40(2) | 50(0) | 178(6) | | 248(6) | |
| | | | | | 9(0) | 34(0) | 204(1) | | | |
| | | | | | | 34(1) | 450(2) | | | |
| | | | | | | | 179(2) | | | |
| | | | | | | | 479(3) | | | |
| Area lost ($m^2$) 1994 | 28(1) | | N.D. | N.D. | 5(1) | 3(0) | 489(0) | | | N.D. |
| | | | | | | 2(3) | | | | |
| Area lost ($m^2$) 1995 | | | N.D. | N.D. | 49(0) | | | | | N.D. |
| N | 2 | 0 | 0 | 0 | 7 | 9 | 10 | 0 | 2 | 1 |
| Sum | 72 | 0 | 0 | 0 | 256 | 230 | 3043 | 0 | 490 | 936 |
| Mean | 36 | 0 | 0 | 0 | 37 | 26 | 304 | 0 | 245 | 936 |
| Standard deviation | 11 | 0 | 0 | 0 | 48 | 25 | 161 | 0 | 4 | |
| Return interval | 585 | 0 | 0 | 0 | 167 | 130 | 117 | 0 | 585 | 1170 |

Values in parentheses indicate number of days following low flow.

and also the inconsistent frequency of rapid-failure events, still escape detailed description, however. When applied to longer-term sandbar erosion, photoanalysis suggests that the diurnal flow cycle nicks and steepens the toe slope of sandbars in a relatively narrow near-river zone (the hydrologically active zone (HAZ) of Kaplinski et al.). Over time, repeated over-steepening of the sandbar toe promotes the downslope movement of subaerial sand from higher portions of the sandbar toward the river.

Our photo measurements are in basic agreement with the Kaplinski et al. (1996) topographic surveys for nine of eleven sandbars. Even though direct comparison of raw area values is not possible (because of differing definitions of baseline sandbar area), both studies suggest that sandbars are variable in size and shape and have not been entirely stabilized by the Interim Flow Prescription. Partitioning the rapid-failure photo data into annual time steps, however, reveals far fewer events in the 1994 and 1995 period than in 1992 and 1993, yet the flow regime appears to be the same. This suggests that either failure events are not strictly correlated with flow regime or sandbars may have been approaching more stable configurations from a mass-flux standpoint toward the end of the study period and before the controlled flood of 1996. The sediment mobilized by both rapid failure and longer-term erosion may be moved into the main channel, or stored in eddies, or some combination of these phenomena. In any event, the significance of high-frequency sandbar reworking is that it increases the opportunity for sediments to enter the main channel. Every time sediment moves into the main channel, the chance for further downstream transport toward Lake Mead is also enhanced.

### Temporal and Spatial Trends of Failure Events

The most frequent recurrence-interval was 117 days for 172.3L, whereas the longest was 1170 days for 212.9L (Table 4). The mean recurrence-interval was 503 days. Erosional events were not uniformly distributed with respect to time or space. For example, during September 1992, eight erosional events occurred at six sites (2.6L, 43.1L, 136.6L, 172.3L, 211.3L, and 212.9L). Three deposits were eroded synchronously on January 30, 1993 (145.5L, 172.2L, and 172.5L). On several occasions during the study, two sites experienced erosion on the same day. Synchronous erosional events occurring at proximal locations suggest that localized channel processes, such as the movement of sediment pulses, may be the trigger for rapid erosional events (as with the previously described separation-eddy feedback). On the other hand, synchronous erosional events occurring at distant locations suggest that a change in discharge pattern may be the triggering mechanism.

Attempts to correlate sandbar characteristics and dynamics to downriver distance were largely unsuccessful. The coefficient of variation is the only parameter that shows any trend suggesting that sandbar area becomes less variable downstream. A slightly more productive approach to systematizing the overall results spatially relates sandbar characteristics to geomorphology. A simple analysis of this relationship was done, using three ordinal classes of general inner-canyon width at each study sandbar (1 = narrow, 2 = medium, 3 = wide). Comparing width to mean sandbar area yields a Spearman's Rho of .360. Comparing width to coefficients of variability yields a Rho of .462. Comparing width to event size yields a Rho of .329, but number of events yields a Rho of only –.006. It appears that the morphometry of the inner canyon and of the channel itself will need to be developed more quantitatively in order to pursue this approach further.

## Conclusions

Sandbar erosion in Grand Canyon appears to proceed in two modes. The first is a "gradual" mode where small quantities of sediment, too small to detect as an "event," erode over time scales of days to weeks. Second, an "event" mode often occurs. In this case, failure of the sandbar along the channel-proximal edge moves significant amounts of sediment from subaerial storage to subaqueous storage in eddies or as transported load in the main channel. These events can occur over time scales as short as a few hours and can display very large instantaneous lateral erosion rates. The greatest number of rapid failures is correlated to sudden or prolonged periods of discharge reduction. Such discharge reduction occurs commonly in the form of weekend low flows or as between-season, multi-day reductions in flow. The Interim Flow Prescription has reduced, but not eliminated, overall sandbar erosion. Partitioning the rapid-failure photo data into annual time steps reveals far fewer events in the 1994 and 1995 period than in 1992 and 1993, yet the flow regime appears to be the same.

If the "dynamic-mass constant-form" definition of stability is accepted, it would appear that there should be little concern about these demonstrations of sandbar degradation in the Grand Canyon, for one would simply assume the sandbars will reform as they have in the past. The shortcoming of applying the "dynamic mass-constant form" definition of stability to Grand Canyon sandbars is that it assumes, indeed requires, mass balance equilibrium where sediment supply is assured. As mentioned earlier, one of the well-documented concerns with managing Colorado River sandbars is the inadequacy of sediment replenishment from tributaries. Given this concern, a low mass-flux definition of stability makes more sense. While operational achievement of such a goal is not reasonable, it is probably appropriate as a management target given the limited sediment input to the system. If the conservation of sediment within Grand Canyon is considered important, the understanding and minimization of these rapid-failure events should be increased, and the phenomenon needs to be addressed in any comprehensive sediment management plan.

We have demonstrated that Grand Canyon sandbars can change dramatically as a result of incompletely understood patterns set up in the diurnal discharge from Glen Canyon Dam. It is a well-documented concept in fluvial geomorphology that as one progresses from the divide downslope toward the channel, the dynamic nature of processes and the rate of change in the resulting landforms increase (Chorley et al. 1984). The findings presented in this study certainly fit well into this conceptual model. As one moves closer to the channel, the rate of sampling needs to be increased to capture the complex nature of processes involved. This implies that daily monitoring needs to be carried out to understand daily changes. The recommendation for intense sampling presents a dilemma to researchers and resource managers alike. The increase in research traffic along the Colorado has not gone unnoticed by park visitors. We, as researchers, should not consider ourselves exempt from the mission and goals of the National Park Service. The methods described here provide a relatively nonintrusive tool for the monitoring of several environmental variables at the required temporal resolution.

## Acknowledgments

We wish to thank the following agencies and individuals: The National Park Service provided funding support. Dave Wegner and others on the Glen Canyon Environmental Studies staff provided direct and in-kind support for this project. Mike Applegarth, Kyle Bohnensteil, Randy Botts, Glenn Dunno, Merrianne Etter, Mark Manone, and Rob Weber performed the image analyses. Larry Stevens, Merrianne Etter, and Liz Boussard reviewed versions of the manuscript. We also wish to thank the reviewers for very useful improvements to the manuscript. The listing of specific brand names of equipment or software is in no way official endorsement of those products.

## References

Andrews, E.D. 1991. Sediment Transport in the Colorado River Basin. In *Colorado River Ecology and Dam Management: Proceedings of a Symposium, May 24–25, 1990, Santa Fe, New Mexico*, pp. 54–74. Washington, DC: National Academy Press.

Bauer, B.O., and Schmidt, J.C. 1993. Waves and Sandbar Erosion in the Grand Canyon: Applying Coastal Theory to a Fluvial System. *Annals of the Association of American Geographers* 83:475–97.

Beus, S.S. 1992. *Colorado River Investigations.* Flagstaff, AZ: Northern Arizona University.

——— and Avery, C.C. 1992. *The Influence of Variable Discharge Regimes on Colorado River Sandbars below Glen Canyon Dam.* Final report. Flagstaff, AZ: Glen Canyon Environmental Studies.

Budhu, M.R. 1992. Mechanisms of Erosion and a Model to Predict Seepage-Driven Erosion Due to Transient Flow. In *The Influence of Variable Discharge Regimes on Colorado River Sandbars below Glen Canyon Dam*, ed. S. Beus and C. Avery, pp. 1–75. Flagstaff, AZ: Glen Canyon Environmental Studies.

——— and Gobin, R. 1994. Instability of Sandbars in Grand Canyon. *Journal of Hydraulic Engineering* 120:919–33.

Carpenter, M.C.; Carruth, R.L.; Fink, J.B.; Boling, J.K.; and Cluer, B.L. 1995. *Hydrogeology and Deformation of Sandbars in Response to Fluctuations in Flows of the Colorado River in the Grand Canyon, Arizona.* Water-Resources Investigations Report 95-4010. Tucson, AZ: U.S. Geological Survey.

Carpenter, M.C.; Carruth, R.L.; and Cluer, B.L. 1991. Beach Erosion and Deformation Caused by Outward Flowing Bank Storage Associated with Fluctuating Flows along the Colorado River in the Grand Canyon. *EOS (Transactions of the American Geophysical Union)* 72:222.

Chorley, R.J.; Schumm, S.A.; and Sugden, D.E. 1984. *Geomorphology*. London: Methuen & Co.

Cluer, B.L. 1992. Daily Responses of Colorado River Sand Bars to Releases from Glen Canyon Dam, 1990–1991: Instantaneous Erosion and Dependent Deposition. In *The Influence of Variable Discharge Regimes on Colorado River Sandbars below Glen Canyon Dam*, ed. S. Beus and C. Avery, ch. 5. Flagstaff, AZ: Glen Canyon Environmental Studies.

———. 1995. Cyclic Fluvial Processes and Bias in Environmental Monitoring, Colorado River in Grand Canyon. *Journal of Geology* 103:411–21.

——— and Dexter, L.R. 1994. *Daily Dynamics of Grand Canyon Sandbars; Monitoring with Terrestrial Photogrammetry*. Final report. Flagstaff, AZ: Glen Canyon Environmental Studies.

———; Carpenter, M.C.; Martin, L.J.; Wondzell, M.A.; Dexter, L.R.; and Manone, M.F. 1993. Rapid Erosion and Slow Redeposition of Sand Bars along the Regulated Colorado River in the Grand Canyon. *EOS (Transactions of the American Geophysical Union)* 74:321.

Collier, M.; Webb, R.H.; and Schmidt, J.C. 1996. *Dams and Rivers: Primer on the Downstream Effects of Dams.* U. S. Geological Survey Circular 1126. Denver: U. S. Geological Survey.

Davis, W.M. 1899. The Geographical Cycle. *Geographical Journal* 14:481–504.

———. 1902. Base-level, Grade and Peneplain. *Journal of Geology* 10:77–111.

Dawdy, D.R. 1991. Hydrology of Glen Canyon and Grand Canyon. In *Colorado River Ecology and Dam Management: Proceedings of a Symposium, May 24–25, 1990, Santa Fe, New Mexico,* pp. 40–53. Washington, DC: National Academy Press.

Dexter, L.R., and Cluer, B.L. 1996. *Extension Study: Daily Dynamics of Grand Canyon Sandbars; Monitoring with Terrestrial Photogrammetry.* Final report. Flagstaff, AZ: Glen Canyon Environmental Studies.

Dolan, R.; Howard, A.D.; and Gallenson, A. 1974. Man's Impact on the Colorado River in Grand Canyon. *American Scientist* 62:393–401.

ERDAS Inc. 1992. P.C. *ERDAS V.7.5 Software, Users Guide and Technical Manual*. Atlanta: ERDAS.

Gilbert, G.J. 1876. The Colorado Plateau Province as a Field for Geological Study. *American Journal of Science* 12:16–24, 85–103.

———. 1877. *Report on the Geology of the Henry Mountains*. U. S. Geographical and Geological Survey of the Rocky Mountain Region. Washington, DC: U. S. Government Printing Office.

Graf, W.L. 1985. The Colorado River: Instability and Basin Management. *Resource Publications in Geography*. Washington, DC: Association of American Geographers.

———. 1992. Science, Public Policy and Western American Rivers. *Transactions of the Institute of British Geographers*. N. S. 17:5–19.

———. 1996. Geomorphology and Policy for Restoration of Impounded American Rivers: What Is "Natural"? In *The Scientific Nature of Geomorphology*, ed. B.L. Rhoads and C.E. Thorn, pp. 443–73. New York: John Wiley & Sons.

Hack, J.T. 1960. Interpretation of Erosional Topography in the Humid Temperate Regions. *American Journal of Science,* Bradley vol. 263A:80–97.

———. 1975. Dynamic Equilibrium in Landscape Evolution. In *Theories of Landform Development,* ed. W. N. Melhorn and R.C. Flemal, pp. 87–102. Boston: Allen & Unwin.

Howard, A.D. 1975. Establishment of Benchmark Study Sites along the Colorado River in Grand Canyon National Park for Monitoring of Beach Erosion Caused by Natural Forces and Human Impact. University of Virginia Grand Canyon Study, Technical Report 1.

——— and Dolan, R. 1979. Changes in the Fluvial Sandbars of the Colorado River in the Grand Canyon Caused by Glen Canyon Dam. In *Proceedings of the First Conference on Scientific Research in the National Parks,* vol. 2, pp. 845–51, New Orleans, LA, November 9–12, 1976. National Park Service Transactions and Proceedings Series 5.

——— and ———. 1981. Geomorphology of the Colorado River in the Grand Canyon. *Journal of Geology* 89:269–98.

Ingram, H.; Tarlock, D.A.; and Oggins, C.R. 1991. The Law and Politics of the Operation of Glen Canyon Dam. In *Colorado River Ecology and Dam Management: Proceedings of a Symposium*, May 24–25, 1990, Santa Fe, New Mexico, pp. 10–27. Washington, DC: National Academy Press.

Johnson, R.R. 1991. Historic Changes in Vegetation along the Colorado River in Grand Canyon. In *Colorado River Ecology and Dam Management: Proceedings of a Symposium*, May 24–25, 1990, Santa Fe, New Mexico, pp. 178–206. Washington: National Academy Press.

Kaplinski, M.; Hazel, Jr., J.E.; and Beus, S.S. 1996. *Monitoring the Effects of Interim Flows from Glen Canyon Dam on Sandbars in the Colorado River Corridor, Grand Canyon National Park.* Final report. Flagstaff, AZ: Glen Canyon Environmental Studies.

Kieffer, S.W. 1985. The 1983 Hydraulic Jump in Crystal Rapid: Implications for River-Running and Geomorphic Evolution in the Grand Canyon. *Journal of Geology* 93:385–406.

Langbein, W.B., and Leopold, L.B. 1964. Quasi-Equilibrium States in Channel Morphology. *American Journal of Science* 262:782–94.

Leopold, L.B. 1991. Closing Remarks. In *Colorado River Ecology and Dam Management: Proceedings of a Symposium*, May 24–25, 1990, Santa Fe, New Mexico, pp. 254–57. Washington, DC: National Academy Press.

——— and Langbein, W.B. 1962. The Concept of Entropy in Landscape Evolution. U.S.G.S. Professional Paper 500-A. Washington: U. S. Government Printing Office.

National Academy of Science. 1987. *River and Dam Management: A Review of the Bureau of Reclamation's Glen Canyon Environmental Studies*. Washington, DC: National Academy of Science.

Schmidt, J.C. 1990. Recirculating Flow and Sedimentation in the Colorado River in Grand Canyon, Arizona. *Journal of Geology* 98:704–24.

——— and Graf, J.B. 1990. Aggradation and Degradation of Alluvial Sand Deposits, 1965 to 1986, Colorado River, Grand Canyon National Park, Arizona. U.S. Geological Survey Professional Paper 1493. Washington: U. S. Government Printing Office.

Schumm, S.A. 1977. *The Fluvial System.* New York: John Wiley and Sons.

Smillie, G.M.; Jackson, W.L.; and Tucker, D. 1993. Colorado River Sand Budget: Lees Ferry to Little Colorado River. National Park Service Technical Report NPS/NRWRD/NRTR-92/12.

Stevens, L.E. 1991. *The Colorado River in Grand Canyon, a Guide.* Flagstaff, AZ: Red Lake Books.

Thorn, C.E., and Welford, M.R. 1994. The Equilibrium Concept in Geomorphology. *Annals of the Association of American Geographers* 84:666–96.

U. S. Bureau of Reclamation. 1995. *Operation of Glen Canyon Dam: Final Environmental Impact Statement.* Washington, DC: U.S. Government Printing Office.

U. S. National Park Service (NPS). 1989. *Colorado River Management Plan.* Grand Canyon National Park report, Grand Canyon, AZ.

Valdez, R.A., and Williams, R.D. 1993. Icthyofauna of the Colorado and Green Rivers in Canyonlands National Park. In *Proceedings of the First Biennial Conference on Research in Colorado Plateau National Parks*, Flagstaff, AZ, July 22–25, 1991, pp. 2–22. Transactions and Proceedings Series NPS/NRNAU/NRTP-93/10. U.S.NPS, U.S. Department of the Interior, Denver.

Weatherford, G.D., and Brown, F.L., eds. 1983. *New Courses for the Colorado River.* Albuquerque: University of New Mexico Press.

Webb, R.H. 1996. *Grand Canyon: A Century of Change*. Tucson: University of Arizona.

Wegner, D.L. 1991. A Brief History of the Glen Canyon Environmental Studies. In *Colorado River Ecology and Dam Management: Proceedings of a Symposium*, May 24–25, 1990, Santa Fe, New Mexico, pp. 226–38. Washington, DC: National Academy Press.

Werrell, W.; Inglis Jr., R.; and Martin, L., 1993. Geomorphic Stability Of Sandbar 43.1L on the Colorado River in the Grand Canyon in Response to Ground Water Seepage during Fluctuating Flow Releases from Glen Canyon Dam. Fort Collins, CO: National Park Service, Natural Resources Technical Report 92/10.

Williams, G.P., and Wolman, M.G. 1984. Downstream Effects of Dams on Alluvial Rivers. U.S.G.S. Professional Paper 1286. Washington: U. S. Government Printing Office.

*Correspondence:* Department of Geography, Northern Arizona University, Box 15016, Flagstaff, AZ 86011, e-mail lrd@alpine.for.nau.edu (Dexter); Water Resources Division, National Park Service, 1201 Oak Ridge Drive, Suite 250, Fort Collins, CO 80525 (Cluer).